



Frans Ritala

## **3D stress state change monitoring using displacement measurements**

Master's thesis, which has been submitted for Master of Science degree.

Espoo, 10.8.2015

Supervisor: Prof. Mikael Rinne

Advisor: M.Sc Topias Siren



---

**Tekijä** Frans Ritala

---

**Työn nimi** Kolmiulotteisen jännityskentän muutoksen seuranta venymämittauksilla

---

**Laitos** Yhdyskunta- ja ympäristötekniikan laitos

---

**Professori** Kalliomekaniikka

---

**Professuurikoodi** Rak-32

---

**Työn valvoja** Professori Mikael Rinne

---

**Työn ohjaaja(t)** Diplomi-insinööri Topias Siren

---

**Päivämäärä** 10.8.2015

---

**Sivumäärä** 82 +4

---

**Kieli** Englanti

---

## Tiivistelmä

Tämän diplomityön tarkoituksena oli koestaa Tekesin Green Mining -hankkeen Dynamine-projektissa kehitettyä jännitystilaa mallintavaa algoritmia. Kokeet suoritettiin Bolidenin Kylylahden kaivoksella, kahdessa erillisessä koejärjestelyssä. Koealueet mallinnettiin ensin Rocsciencen Examine – ohjelmilla. Tämä tehtiin, jotta instrumentointi olisi mahdollisimman kattavaa. Koealueille asennettiin yhteensä 14 extensometria.

Ennen varsinaisia data-analyyskejä algoritmia koestettiin Examine2D - ohjelmalla luodulla synteettisellä datalla. Näin varmennettiin tässä tutkimuksessa käytetyt mallinnusratkaisut. Synteettinen koestaminen tehtiin kolmessa erillisessä osassa. Ensimmäisessä osassa käytettiin kaukokenttämallinnusta, toisessa lähikenttämallinnusta ja viimeisessä osassa laskentaan otettiin mukaan leikkausjännitys.

Seuraavassa vaiheessa mitatut siirtymät muunnettiin venymiksi. Tämän jälkeen tarkasteltiin louhinnan aiheuttamaa vaikutusta kalliomassaan. Tarkastelun perusteella tutkitavan datan määrää kavennettiin.

Algoritmillä analysoitiin vain 2D koealue. Kuten synteettisellä datalla, myös oikealla datalla koealue mallinnettiin sekä kaukokenttämallinnuksella että lähikenttämallinnuksella. Analyysista saadut tulokset eivät olleet suurusluokaltaan realistisia. Joidenkin mittausten osalta sopivuus mitattujen ja arvioitujen venymien suhteen oli hyvä, mutta näidenkin mittausten osalta tulosten suurusluokka oli väärä. Mittausvirheiden eliminointiseksi työssä analysoitiin myös Posivan ONKALOSTA kerättyä mittausdataa, mutta myös tämän datan kanssa tulosten suurusluokka oli väärä.

Työn viimeisessä osassa käydään läpi tuloksiin vaikuttaneita tekijöitä. Suurimpia tuloksiin vaikuttavia tekijöitä olivat extensometrejä läpäisevät rakolinjat, kalliomassan kimmomoduuli sekä häiriintynyt kalliomassa, mittaustavasta johtuneet epätarkkuudet ja mallinnustavasta johtuneet epätarkkuudet. Työssä esitetään myös parannusehdotuksia tuleviin koejärjestelyihin.

---

**Avainsanat** Kalliomekaniikka, takaisinlaskenta, jännitystila, venymä, online mittaukset, extensometri, superpositio periaate, instrumentointi

---



---

**Author** Frans Ritala

---

**Title of thesis** 3D Stress State Change Monitoring Using Displacement Measurements

---

**Department** Department of civil and environmental engineering

---

**Professorship** Rock mechanics

---

**Code of professorship** Rak-32

---

**Thesis supervisor** Professor Mikael Rinne

---

**Thesis advisor(s) / Thesis examiner(s)** M.Sc Topias Siren

---

**Date** 10.8.2015

---

**Number of pages** 82+4

---

**Language** English

---

## **Abstract**

The purpose of this Master's thesis is to test stress estimation algorithm created in Tekes Green Mining Programs Dynamine project. The test were conducted in Boliden Kylylahti mine and included two different test sites. The test sites were first modelled using Rocscience Examine2D and Examine3D to enable comprehensive positioning of used instruments. In total 14 extensometers were installed to the mine.

Prior to real data analysis the algorithm was tested using synthetic data created with Examine 2D program. This was done to ensure that the modelling selections done for this study were adequate for the algorithm to be used. The testing with synthetic data was divided into three separate parts: analysis with far field modelling, near field modelling and with shear stress.

The data received from the measurements was first converted from displacements to strains. After this the rock mass response of each of the test sites were examined. Based on these examinations the amount of data was narrowed down.

The actual analysis were only conducted to the 2D test site. As with synthetic data analysis, the analysis were done for both near and far field. The results from the analysis were not in realistic magnitude. For some measurements good fits were found between measured and estimated strains. To eliminate possible measurements errors also data received from Posiva's ONKALO test was analyzed but the results were similar to results gained from Kylylahti mine.

In the last part of the study reasons affecting to the results were covered. The main reasons were joints passing thru extensometers, rock mass modulus and disturbed rock mass, measurement inaccuracies caused by the used measurement equipment and inaccuracies caused by the used modelling software. Also improvements for further research were stated.

---

**Keywords** Rock mechanics, back calculation, stress , strain, online measurements, multiple linear regression, extensometer, superposition principle, instrumentation

---



## Acknowledgements

*This Thesis will be my final project done for the Aalto University, at least for now, and it marks an end of era for me. It has been quite an experience to study and work at the Aalto University and I am leaving with gratitude, experience and knowledge.*

*First of all, I would like to thank the participants of the Dynamine project for funding and making my Thesis possible. I would also like to thank Topias Siren who has been active commenter and support for my thesis and Professor Mikael Rinne for giving me this opportunity and for his support. The help from Boliden Kylylahti has also been valuable and I would like to express my gratitude towards Eero Tommila and Antti Sorsa. I have also received help from colleagues and I want to especially thank Lauri Uotinen for helping me with all sorts of problems.*

*I also want to express my gratitude for the support I have received from home. Thanks, Susanna!*

*Finally, I would like to thank Stepan who unfortunately was not around to see his work to be finished.*

Frans Ritala

Espoo 20.7.2015

## Table of Contents

Table of Contents.....	1
List of figures .....	3
List of tables .....	5
List of symbols .....	6
1 Introduction.....	7
1.1 Background .....	7
1.2 Objectives.....	7
1.3 Experiment .....	8
2 Methods.....	11
2.1 Basic principles of this study.....	11
2.2 Inversion problem.....	12
2.3 Inversion back-calculation .....	12
2.4 Weaknesses of the back-calculation method.....	15
2.5 Near and far field modelling .....	16
2.6 Mining efficiency and safety improvement methods .....	16
3 Experiment site and <i>in situ</i> conditions .....	20
3.1 In situ conditions .....	20
3.2 Preliminary modelling .....	23
3.3 Experiment instrumentation .....	31
3.4 Instruments .....	31
3.5 Installation procedure.....	34
4 Verification of the back calculation method.....	37
4.1 Synthetic 2D analysis.....	37
4.2 2D synthetic analysis with near field modelling .....	41
4.3 2D synthetic analysis with shear stress.....	42
5 Monitoring and back calculation results .....	45
5.1 Executed excavations.....	45
5.2 Rock mass response of 2D test site.....	48

5.3	Rock mass response of 3D test site.....	50
5.4	Preparation of the data .....	51
5.5	2D analysis with far field modelling.....	53
5.6	2D analysis with near field modelling .....	57
5.7	2D near field analysis of the Posiva 2011 test site .....	61
6	Discussions .....	70
6.1	Joints .....	70
6.2	Rock mass modulus and Poisson ratio.....	73
6.3	Used measurement equipment.....	75
6.4	Modelling and software used for the modelling.....	76
6.5	Improvements for installation procedure .....	77
7	Conclusions.....	79
	References .....	81
	Appendices .....	83
	Appendix 1: Total displacements and the comparison displacements .....	83
	Appendix 2: Measured strains from Kylylahti mine .....	83
	Appendix 3: Measured displacements from ONKALO.....	84
	Appendix 4: Used algorithm .....	84



## List of figures

Figure 1. Location of Boliden Kylylahti mine. ....	9
Figure 2. Location of test site at level 322. ....	9
Figure 3. Process chart of using the algorithm. ....	15
Figure 4. Near and far field modelling. a) near field model an b) far field model .....	16
Figure 5. Stress failure paths. (Kaiser, Yazici & Maloney 2001.) .....	18
Figure 6. Cross-section of the Kylylahti mine ore zones and the locations of the test sites. (Picture given by Boliden Kylylahti) .....	21
Figure 7. Cross-section of the level 322 test site. On the left the area to be mined. ....	24
Figure 8. Modelled differential stresses before excavation of the stope.....	26
Figure 9. Modelled differential stresses after excavation of the stope .....	26
Figure 10. Rhinoceros model of the level 410 test site. Excavation target marked with red and the measurement site with blue arrow. a) from North and b) from East. ....	29
Figure 11. Structure of the SMART MPBX. (Tod J. & Lausch P.) .....	32
Figure 12. Measurement site before installation of the extensometers.....	34
Figure 13. Location and direction measurement of the drillhole .....	35
Figure 14. Installed extensometers presented with Examine2D. ....	36
Figure 15. Locations of the extensometers at level 420.....	36
Figure 16. Forming method of the load cases. a) Load case $\sigma_{xx}$ , b) load case $\sigma_{yy}$ and c) load case $\tau_{xy}$ . ....	38
Figure 17. Mohr`s circle example of shear stress load case.....	39
Figure 18: Example of the near field model.....	41
Figure 19. Estimated strain difference against "measured" strain difference with synthetic data.....	44
Figure 20. Rock units under the excavated area. 3DEC model. (Picture given by Boliden Kylylahti) .....	45
Figure 21. Target excavation on level 410 sequenced mining and dates from 2D perspective.....	47
Figure 22. Strains of EXT-14 located at the test site 1. ....	48
Figure 23. Plastic deformation example (0 to 2m). ....	51
Figure 24. Plot of the results of the 2D far field analysis at the Kylylahti mine against time. Stresses in MPa and angle in degrees. ....	55
Figure 25. Estimated strain difference versus measured strain difference. 9.3.2015. Extensometers marked with different colors.....	56

Figure 26. Estimated strain difference versus measured strain difference. 22.1.2015. Extensometers marked with different colors.....	56
Figure 27. Near field analysis results against time. ....	59
Figure 28. Measured strain 9 <sup>th</sup> of March versus estimated strain with near field analysis. Extensometers marked with different colors.....	59
Figure 29. Measured strain 22 <sup>nd</sup> of January versus estimated strain with near field analysis. Extensometers marked with different colors. ....	60
Figure 30. Time frame of interest of the Posiva measurements. Extensometers marked with E_EX and temperature measurements as T_EX. (Siren T. 2013) .....	62
Figure 31. Modelled stages at the Posiva test site. ....	65
Figure 32. Posiva test site results against time. ....	68
Figure 33. The fit on 1 <sup>st</sup> of November 2011 between measured and estimated strains. Extensometers marked with different colors.....	68
Figure 34. The fit on 27 <sup>th</sup> of October 2011 between measured and estimated strains. Extensometers marked with different colors.....	69
Figure 35. Impact of joint to multipoint borehole extensometer. ....	71
Figure 36. Joint example. Joint causing the curvature due to the fact that most of the displacements are in on place. ....	72
Figure 37. Effect of joint in rock mass presented as one-dimensional spring. ....	73

## List of tables

Table 1. Rock properties of Kylylahti mine rock units based on information received from Boliden Kylylahti. ....	22
Table 2. Modelling parameters.....	25
Table 3. Displacements before excavation of the target stope. The locations where extensometers were planned to install are on bold. ....	28
Table 4. Strain calculations from the Examine2D model. Y1, Y2, X1 and X2 are coordinates of the extenometer.....	40
Table 5. Example data set of measured displacements from the Kylylahti. ....	52
Table 6. Strains from the 2D test site at the Kylylahti mine. Extensometer EXT-14. ....	53
Table 7. Multiple linear regression multipliers obtained from the Kylylahti Mine data.	54
Table 8. Final results of the far field analysis of the Kylylahti mine data .....	55
Table 9. Multiple linear regression results of the Kylylahti mine data for the near field analysis.....	57
Table 10. Final results of the near field analysis. ....	58
Table 11. Strains of the chosen measured displacements. ....	63
Table 12. Modelling parameters for the Posiva test site. (Hakala. Valli. 2013. p. 7).....	64
Table 13: Modelled strains for the Posiva test site. $\sigma_1$ .....	65
Table 14. Modelled strains for the Posiva test site. $\sigma_3$ .....	65
Table 15. Modelled strains for the posiva test site. Tau .....	66
Table 16. Beta factors of the multiple linear regression analysis of the Posiva data. ....	67
Table 17. Final results of the Posiva test site near field analysis. ....	67

## List of symbols

D		Disturbance factor
$E_i$	[GPa]	Intact rock deformation modulus (Young's modulus)
$E_m$	[GPa]	Rock mass deformation modulus
I	[A]	Electric current
R	[ $\Omega$ ]	Resistance
U	[V]	Voltage
UCS	[MPa]	Uniaxial compressive strength
l	[mm]	Length
$m_i$		
$\nu$		Poisson's ratio
$\varepsilon$		Strain (engineering strain)
$\rho$	[Kg/m <sup>3</sup> ]	Density
$\sigma$	[MPa]	Principal stress
$\tau$	[MPa]	Shear stress
$\theta$	[ $^\circ$ ]	Angle between principal stresses

# 1 Introduction

## 1.1 *Background*

This Master's thesis is part of Tekes Green Mining -programmes Dynamine research project. The purpose of this study is to describe testing of online stress measurement system created in the project. The main aspects of this study are in the implementation of the measurement system into mining conditions and the transition from using synthetic data to real data with the back-calculations.

The strain measurements used in this project are widely used in the mining industry but not usually to monitor stress state change. Stress state change monitoring is able to give feedback about the success of mining sequencing and sufficiency of ground control methods. The current state of the stress monitoring is concentrated on *in situ* stress measurements rather than long-term stress change monitoring. Often the stress state change is only modelled but not measured. With displacement measurements continuous monitoring is more often used.

The objective of this study is to test a tool for the mines to monitor the stress state changes caused by the mining activities. Stress state change monitoring is able to give feedback about the success of mining sequencing and sufficiency of ground control methods. By monitoring the actual change the design and the sequencing of the stopes can turn into an iterative process. With the real-time monitoring of the stress state it is possible to increase the safety of underground mines especially if the stress changes cause significant risks.

## 1.2 *Objectives*

The main object of this study is to test the algorithm developed in the earlier phase of the Dynamine project and to evaluate its suitability for mining environment. During the evaluation process problems associated with using real rock mass are documented. Also

possibilities to vary measurement equipment are investigated. The main goal is to provide information how to improve the usability of the algorithm in mine-like conditions and to find out if the linearly elastic modelling is sufficient for real rock mass.

Often in mining, the rock mechanical knowledge is created with an iterative process and the rock mechanical and the stress model can vary significantly during the life of mine. One of the goals of this study is to test if the algorithm presented in this study is a suitable tool for the iterative process. The stress model is most affected during the life of mine by the mining sequencing and the amount of empty space in the mine. Understanding and controlling the stress state is vital, especially in high stress conditions.

### 1.3 ***Experiment***

The experiment sites of this project are located at Kylylahti Mine. The location of the mine is shown in Figure 1. The first test site for verifying the 2D algorithm is located at the level 322 next to a level 325 where the actual excavations are going to be done. The level is located approximately 400 meters from the surface and it has simple geometry. The cross section of the stope and the installation location are presented in the Figure 2. The extensometers are going to be installed from the tunnel next to the stopes.



**Figure 1. Location of Boliden Kylylahti mine.**

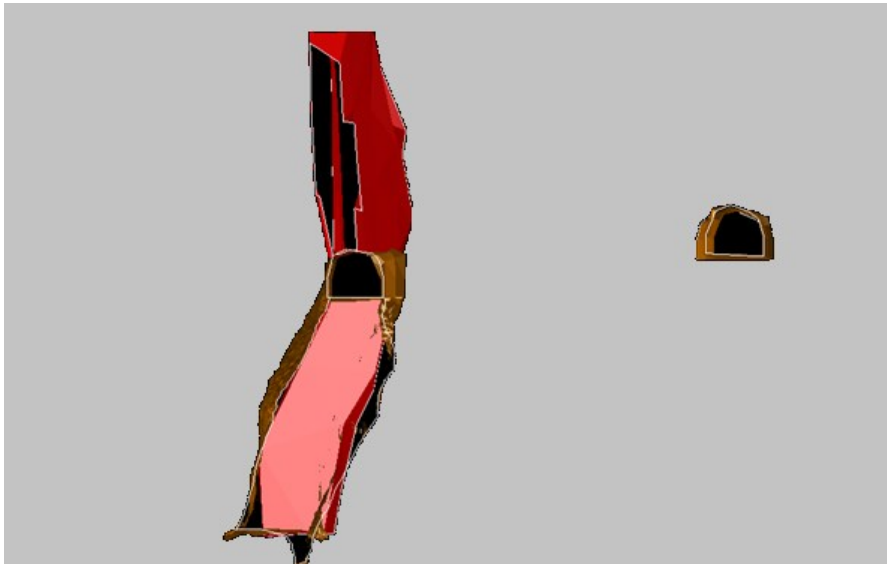


**Figure 2. Location of test site at level 322.**

The 2D test site consists of two extensometers and one datalogger. The test site was measured with dataloggers only for three weeks and after which the extensometers were

read manually. The purpose of this test site is to get real data to verify that the algorithm works sufficiently in areas with simple geometry.

The 3D test site is located at level 410. The test site was established to monitor large stope at depth of 492 meters. Level 410 has more complex geometry and the interpretation of the data received requires 3D modelling. The level has already been partially mined.



## 2 Methods

In this chapter the methods used in this study are presented with basic principles in the chapter 2.1. The theoretical background of this study consists of three main parts. First part is the inversion problem presented in the chapter 2.2. The second part is the statistical method used in the project which is presented in the chapter 2.3. The last part is the mechanical background of this study which is presented in the same chapter.

### 2.1 *Basic principles of this study*

The most important factor in this study is stress. Stress is not a physical phenomenon that can be measured directly. Stress can be determined for finite region based on the measurable displacement it causes for material with known Young's modulus. This principle was presented by Robert Hooke in his anagram *ut tension, sic vis* (As the force, so the force) in 1678.

The stress measurements within rock mechanics can be divided into two different categories, *in situ* stress measurements and stress state change measurements. In this study the main concern is in the stress state change.

The method used in this study uses few simple principles. First of all the stress state change causes displacement in the measured object. This displacement can be measured, unlike the stress state change. When the displacement is measured it can be converted into stress state change using the Young's modulus. This is more extensively explained in chapter 2.3.

The other important principle in this study is the Hooke's law. In Hooke's law the displacement caused by the force is defined via spring coefficient. In this study when modelled unit load displacements and measured displacements are compared and the rock mass is thought to have the same spring coefficient in both. Thus the change in force and in stress can be calculated.

## 2.2 *Inversion problem*

According to Finnish Center of Excellence in Inverse Problem Research typical inversion problem arises from asking simple questions “backwards”. The method is used in many fields of science such as image processing, geophysics and mathematical finance. Typically inverse problems have infinite amount of answers. (Inversion Problem Research. 2015.)

In this study simple question for the inversion problem is “If we know the stresses impacting to the studied area, how does the rock mass move if there is an excavation of certain size implemented in the rock mass?”

The inversion problem in this study is “if we know the displacements in certain rock mass what was the stress state change from the original stress state?”

## 2.3 *Inversion back-calculation*

The inversion back-calculation algorithm created in earlier part of Dynamine project solves the inverse problem presented in the previous chapter. The back-calculation algorithm is created under restriction of linearly elastic medium. The inversion algorithm is presented with comments in Appendix 4.

The algorithm uses measured displacements of the rock mass as input data. The displacements can be measured with any existing method. The required parameters for the algorithm are modulus of elasticity, Poisson’s ratio, major and minor principal stresses and the direction of the stresses.

When calculating the simple direct problem the total strain caused by the change of the loading factors following applies  $\Delta \varepsilon_{tot} = L_z \Delta \varepsilon_{\sigma,z,1} + L_x \Delta \varepsilon_{\sigma,x,1} + L_{xz} \Delta \varepsilon_{\sigma,xz,1}$  where  $\Delta \varepsilon_{tot}$  is total strain difference,  $L_i$  is loading factor for loading component and  $\Delta \varepsilon_{\sigma,i,1}$  strain difference component

is calculated by simulating a bolt with a chosen modelling program. There are multiple methods to simulate the behavior of loaded bolt but in this study boundary element method software is used and the strains are calculated using normal stresses and shear stresses in plane directions. The equations used to simulate the bolts in simple scenario without shear stress are presented as.

$$\sigma_{bolt} = \sin(\alpha) \sigma_{xx} + \cos(\alpha) \sigma_{yy} \quad (1)$$

$$\varepsilon_{bolt} = \frac{\sigma_{bolt}}{E} \quad (2)$$

The goal of the algorithm is to find out the loading factors. In simple case  $\varepsilon_T = \varepsilon_{l,1} L$  where  $\varepsilon_T$  is vector of measured bolt strain data (length N measured data),  $\varepsilon_{l,1}$  is matrix of strain components from according unit loading (size 3 \* N) and L is vector of loading factors for loading components (length 3).

The linear combination which is shown above in equation (3)

uses the same superposition principle to back calculate the stress tensor. The stress tensor is divided into six different matrices and the algorithm finds the best fit for each factor from the acquired data.

$$\begin{bmatrix} \sigma_x & \tau_{xy} & \tau_{xz} \\ \tau_{xy} & \sigma_y & \tau_{yz} \\ \tau_{xz} & \tau_{yz} & \sigma_z \end{bmatrix} = a \begin{bmatrix} \sigma_x & 0 & 0 \\ 0 & 0 & 0 \\ 0 & 0 & 0 \end{bmatrix} + b \begin{bmatrix} 0 & 0 & 0 \\ 0 & \sigma_y & 0 \\ 0 & 0 & 0 \end{bmatrix} + c \begin{bmatrix} 0 & 0 & 0 \\ 0 & 0 & 0 \\ 0 & 0 & \sigma_x \end{bmatrix} \\ + d \begin{bmatrix} 0 & \tau_{xy} & 0 \\ \tau_{xy} & 0 & 0 \\ 0 & 0 & 0 \end{bmatrix} + e \begin{bmatrix} 0 & 0 & \tau_{xz} \\ 0 & 0 & 0 \\ \tau_{xz} & 0 & 0 \end{bmatrix} + f \begin{bmatrix} 0 & 0 & 0 \\ 0 & 0 & \tau_{yz} \\ 0 & \tau_{yz} & 0 \end{bmatrix} \quad (3)$$

Where:

- $\sigma_{1..3}$  Principal stresses
- $\tau$  Shear stress components
- a..f Multipliers for each stress tensor component

The equation changes based on the calculated case. The presented equation is for 3D case with shear strength component. For the 2D analysis without shear strength component only factor  $a$  and  $b$  need to be calculated. For the 2D analysis with shear strength component also the factor  $d$  has to be calculated.

The algorithm uses ordinary least squares method to calculate the optimal fit between the measured and modelled strains.

As result of the algorithm multipliers for each stress tensor component, later referred as Beta factors, are received. These factors are the results gained from the multiple linear regression. After the beta factors have been calculated the results are transformed into principal stresses.

The data gathered from the extensometers is expected to have outliers. The original goal of the algorithm was to have an in build outlier elimination. At the moment the outlier elimination method used in the algorithm has not been seen to be suitable for purpose and it is not to be used in this study. For future implementations of the algorithm suitable outlier elimination system has to be developed.

To automate the code as much as possible it was rewritten for the purposes of real data analysis. The rewrites concentrated on data handling and how to form the used matrices as efficiently as possible. In the past the results gained from the synthetic cases were written into the code but to gain more efficiency the code was changed to read the results from Excel to enable fast examination of multiple chronological cases.

The process of how to implement the algorithm in to mining environment is presented in Figure 3.

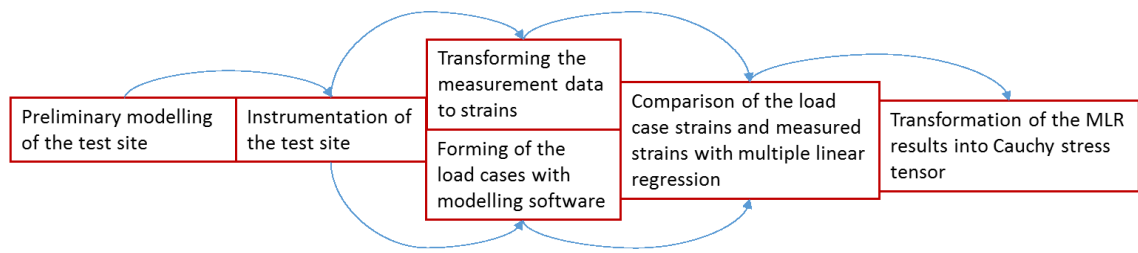


**Figure 3. Process chart of using the algorithm.**

## 2.4 *Weaknesses of the back-calculation method*

The linearly elastic back-calculation method is suitable only when the rock mass is in linearly elastic state. If plastic deformations occur the algorithm produces wrong results. The plastic deformations such as slip failure give bad results because the displacements or strains occur at wrong place and with wrong magnitude. Thus comparing results gained from plastic deformation to linearly elastic model does not give any useful information.

The algorithm was benchmarked with different synthetic data sets to test its weaknesses against different scenarios. These scenarios were data with noise, data with missing points, unknown joint crossing instruments and parallel joint set affecting to the area but not crossing the instruments. Also case where the measurement units were mixed was examined.

With these test it was shown that small amounts of noise or partially missing data do not cause significant errors to the results. The worst results were obtained when a joint with unknown joint parameters was crossing the instruments. In this scenario the results gained with the back-calculation method were differing as much as 75% from the simulated model. This proves that the method is very sensitive for plastic deformations.

## 2.5 *Near and far field modelling*

Two types of modelling are used in this study, near and far field modelling. The difference between these two models is that to the near field model also the structures within close distance to the modelling target, such as stopes and tunnels, are modelled.

The use of near field modelling is necessary when the structures are close enough to cause change to the direction of the stress stage change. This effect can be seen in Figure 4. For this study no accurate near field modelling border was set and it was in the interest of the study to see which of the modelling methods suits for the algorithm better.

The difference between near and far field modelling is presented in Figure 4.

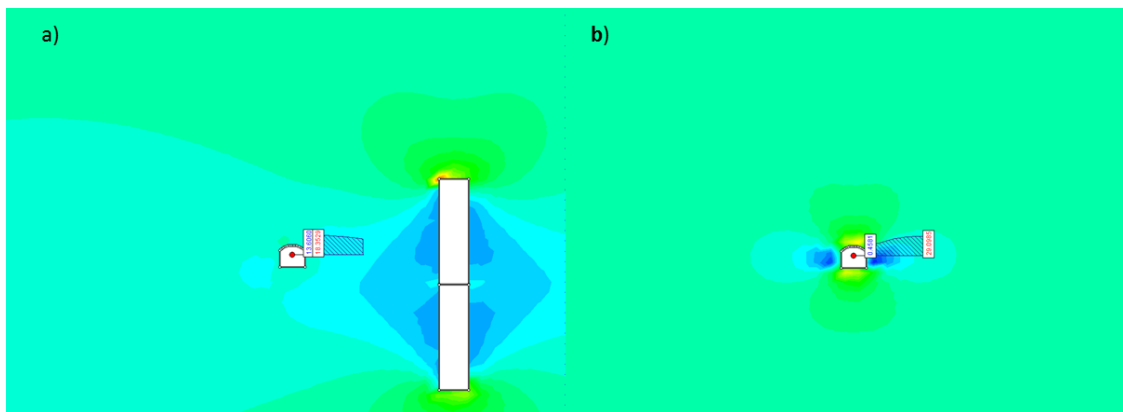


Figure 4. Near and far field modelling. a) near field model an b) far field model

## 2.6 *Mining efficiency and safety improvement methods*

This study covers only stress and rock mechanics related safety and efficiency matters and the purpose of this chapter is to introduce stress and rock mechanics methods which effect on mining efficiency and safety.

The rock mechanical knowledge of a mine can be divided chronological into to four different parts (Hoek, Kaiser & Bawden 2000). The first phase is the exploration phase when only limited amount of rock mechanical data is available. Stress state and stress

model are at this phase based on data gathered from surrounding mines and for example from world stress map and are highly inaccurate.

The second phase is the mine layout design. Some *in situ* stress measurements may have been conducted and detailed geological mapping has been done. During this phase still major uncertainties exist mainly concerning how the mining effects to the stresses and the geological circumstances. (Hoek, Kaiser & Bawden 2000)

During these first two steps many important decisions are made. For example the level spacing, the direction of the stope and the stope size are decided at early stage. These decisions are vital for the mining to be successful and the decisions made at this stage are often also hard to change. (Hoek, Kaiser & Bawden 2000)

The third phase is the first steps in actual mining. This phase involves excavating the accesses to the mine such as shafts or declines and the excavation of the first stopes. During this phase more knowledge is gained how the excavating is effecting to the mined area and how the designed supports are working together with the rock mass. (Hoek, Kaiser & Bawden 2000)

The fourth phase consists of the later years of the mining. During this phase the secondary stopes are mined and the empty space in the mine increases and affects the stresses. During this phase it is essential to know how the rock mass and the stresses behave and what the most important failure models in the mine are. (Hoek, Kaiser & Bawden 2000)

This study mainly concerns on the third and fourth phase and how to increase the knowledge and steepen the learning curve during these phases. The method proposed in this study is intended to give additional information of effects of the mining to the surrounding rock mass, especially to give additional information how the stresses are acting in near the excavations. (Hoek, Kaiser & Bawden 2000)

The importance of the rock mechanical model for the mine is high. Rock or stope failures can cause fatalities, injuries and significant economic losses. The thorough understanding of the rock mechanical model will also help to reduce ore losses and dilution and to optimize the support used for the stopes. Proper rock mechanical knowledge and

research will also improve mines long-term economics while at the same time reducing economical risks.

Rock mechanical models created for the mines are matter of constant improvement. There are ways to validate and get information if the proposed rock mechanical model is suitable for the mine and that the critical points pointed out by the model are the most critical points to be concerned.

In Figure 5 stress related failure modes are presented. The failures can be caused by two different paths. The first path presented in the picture is driven by the relaxation of the rock mass. Relaxation can lead the rock mass to lose its tensile strength. The second path causes stress-driven wedge failures. Wedge failures are caused by the increase of  $\sigma_1$  compared to  $\sigma_3$ . (Kaiser, Yazici & Maloney 2001.)

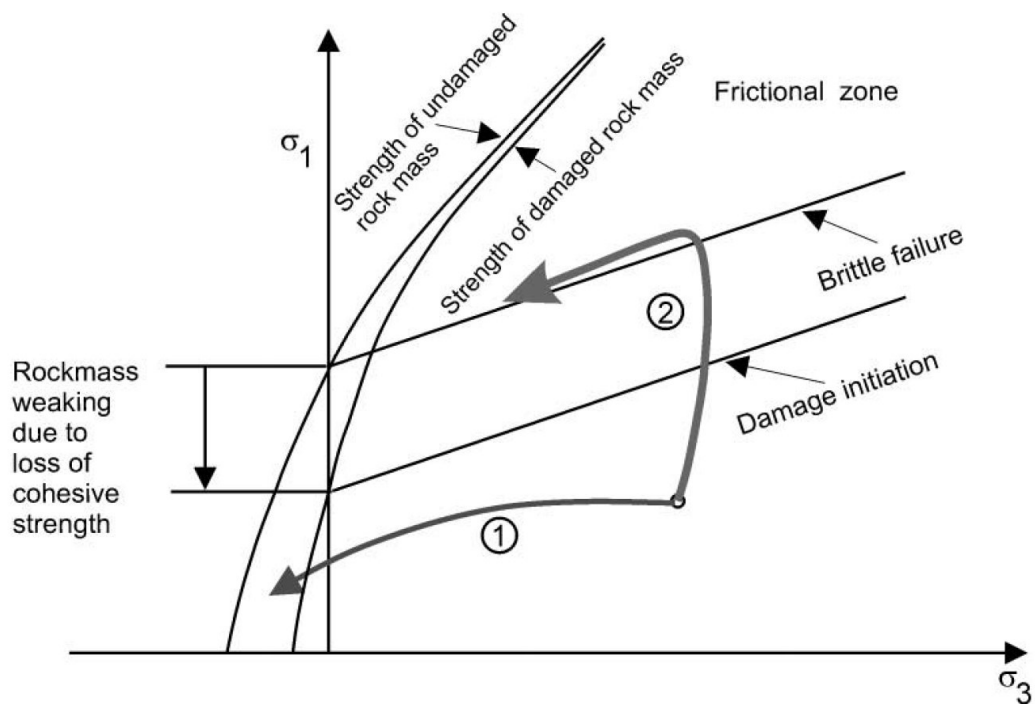


**Figure 5. Stress failure paths. (Kaiser, Yazici & Maloney 2001.)**

The iterative process of gained rock mechanical knowledge is well described in conference paper by Bergström, Sahala and Hakala (2014). In the early stage of the Pyhäsalmi mines deep extension, the main considerations were at the pillar yielding but later changed to ore zone contact where most critical damages occurred.



The goal of this study is to find out if the proposed method can warn the user before the stress has changed to zone which might cause a possible failure.

Currently the stress is rarely monitored at mine sites. Only few examples of time dependent stress monitoring can be found. More often strain of the rock mass is monitored with extensometers in destination that have been determined to be critical.

In coal mining there have been cases where seismic, stress and strain monitoring has been combined and used for monitoring of the longwall face and its displacement and stress state change.

### 3 Experiment site and *in situ* conditions

In this chapter instruments used in this study are covered. The main considerations are concentrated to operation of the instruments for the later analysis and to the installation procedures.

#### 3.1 *In situ* conditions

The information about the test site was given by Boliden Kylylahti. The test site is located at the Kylylahti mine which is located in Eastern Finland. The regional geology at the mine site consists five different geological zones: Outokumpu assemblage ultra-mafic rocks serpentinite and soapstone (the OUM unit), high temperature altered ultra-mafic rocks (OME unit), Kaleva assemblage metasedimentary rocks and massive and semi-massive sulfides.

From geotechnical point of view the geological zones represent also the geotechnical zones with the exception that the semi-massive and massive sulfides have similar properties and can be treated as single geotechnical zone. Between geotechnical zones there is usually a transition zone with varying length. The borders between different zones are not clear.

There is also a separate soapstone unit located at the depth 410 m at the footwall of the ore. The geotechnical properties of this zone vary significantly from the other geological domains and due to the nature of this study this area was to be avoided due to its complexity.

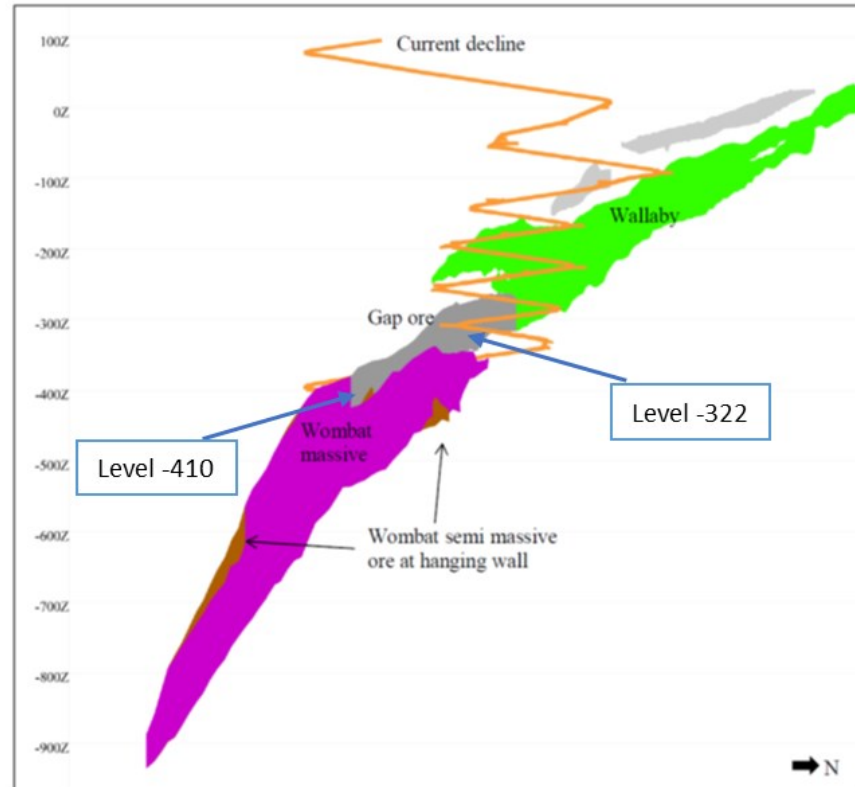


**Figure 6. Cross-section of the Kylylahti mine ore zones and the locations of the test sites. (Picture given by Boliden Kylylahti)**

The orezone at the Kylylahti mine is divided into three different ore domains. The first test site on level 322 is located at the gap ore where the ore body is thinnest. The second test site on level 410 is located at upper part of the wombat massive sulfide ore body.

The rock qualities of different geotechnical domains were determined in previous rock mechanical studies made for Boliden Kylylahti. For this study the OME and MS-SMS (massive and semimassive sulphide unit) units were most important since majority of the extensometers were located within these units. Both of the units have similar Young's modulus but the uniaxial compressive strengths of the units differ by OME being the weaker unit. The exact rock properties are presented in Table 1. Rock properties of Kylylahti mine rock units

**Table 1. Rock properties of Kylylahti mine rock units based on information received from Boliden Kylylahti.**

<i>Rock unit</i>	<i>UCS (MPa)</i>	<i>E (Gpa)</i>	<i><math>\nu</math></i>	<i><math>\rho</math> (kg/m<sup>3</sup>)</i>
<i>KAL</i>	155	60	0.35	2800
<i>MS-SMS</i>	140	85	0.32	3300
<i>OME</i>	95	90	0.32	2900
<i>OUM</i>	150	75	0.33	2800
<i>Soapstone</i>	35	35	0.32	2800

The aspect of rock unit heterogeneity is important for the later parts of the study. The algorithm created in the earlier part of Dynamine project was created for CHILE (continuous, homogeneous, isotropic and linearly elastic) material, homogeneity being one of the important factors to be considered. The heterogeneity/homogeneity of the two important rock classes used in this study was previously investigated at the Kylylahti mine and the results of the investigations were given for this study. The OME unit has clear heterogeneity. The rock unit has clear foliation which will have impact to the displacement measurements. The OME unit includes only few fractures per meter but there are also fault zones included into the zone.

The MS-SMS unit is structure wise similar to OME unit. It has strong heterogeneity and only few fractures per meter. The semi-massive and massive sulphides are mixed with typical host rocks. There is also some foliation but the foliation is not as strong as in the OME unit.

### 3.2 *Preliminary modelling*

The pre-modelling was done to predict results for the actual study and especially to optimize the instrumentation. The first excavation to be modelled is located at the 325 level. The stress state before and after the excavation were modelled to determine the strains caused by the excavation. The pre-modelling was also done to solve the optimal angle for the extensometers. For the optimal angle there is two main criterias. The first criteria is that the displacements are measurable with used equipment. The second criteria is that that angles used in the study vary enough so that both vertical and horizontal displacements are measured.

Rocscience Examine 2D and 3D were chosen to be the used modelling software for this study because it was used already in the previous phase of the Dynamine project. Examine uses boundary element method (BEM) which sets restrictions to the modelling. These restrictions include using of only one rock mass in the model.

The modelling of the 325 level was considered to be difficult since a stope under the stope to be mined had been backfilled recently. Several possibilities for the backfill modelling were thought. The BEM method restricts usage of different materials so different material boundaries for the model were not possible. The problem was solved by modelling the backfill as an empty stope. In a big scale new backfill is thought to act as empty stope since it does not let any significant stresses thru. The typical values of Young's modulus for cemented backfill vary from few hundred MPas to few GPas. These values are significantly lower than the values of intact rock so the modelling of the backfill as empty stope does not have significant difference to the result. The cross-section of the stope is presented in Figure 7.

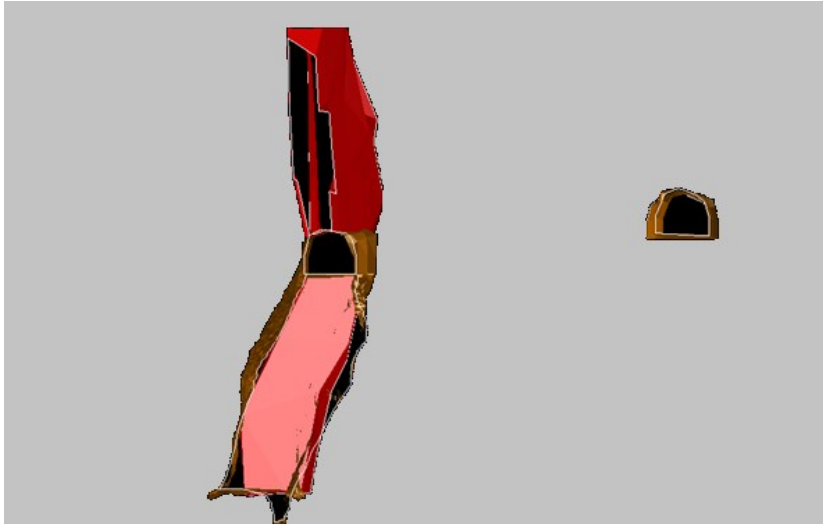


**Figure 7. Cross-section of the level 322 test site. On the left the area to be mined.**

The modelling parameters were acquired from Boliden. The rock mechanical data for the report was gathered from multiple sources. The stress measurements were conducted in 2014 from a depth of 400 meters using LVDT-cell. The rock properties such as uniaxial compressive strength, Young's Modulus, Poisson's ratio and density were averages of laboratory test.

The parameters used in modelling were combined averages of rock units within the monitored area. The actual modelling parameters are shown in Table 2. The Rock Mass Modulus ( $E_m$ ) was calculated with Rockdata and by using Hoek-Brown failure criterion. More information about the used method can be found from article from Hoek and Brown (1997).

**Table 2. Modelling parameters**

<b><i>Modelling parameters</i></b>	<b><i>Value</i></b>	<b><i>Unit</i></b>
$\sigma_1$	30.8	MPa
$\sigma_3$	11.3	MPa
$\sigma_z$	22.5	MPa
$E_m$	29	GPa
$\nu$ (Poisson's ratio)	0.3	
<i>Intact Comp. Strength</i>	110	MPa
<i>GSI</i>	70	
$m_i$	15	
$D$	0.5	

The models created with Examine2D are shown on Figure 8 and Figure 9. 19 data queries were added to the model to represent the extensometers. The queries were added to every five degrees as shown in the Figure 8 and Figure 9.

The first model in Figure 8 represents the situation before the monitored stope is excavated. The model is presented in the picture with differential stresses because the differential stresses are presenting the change caused by the excavation of the stope.

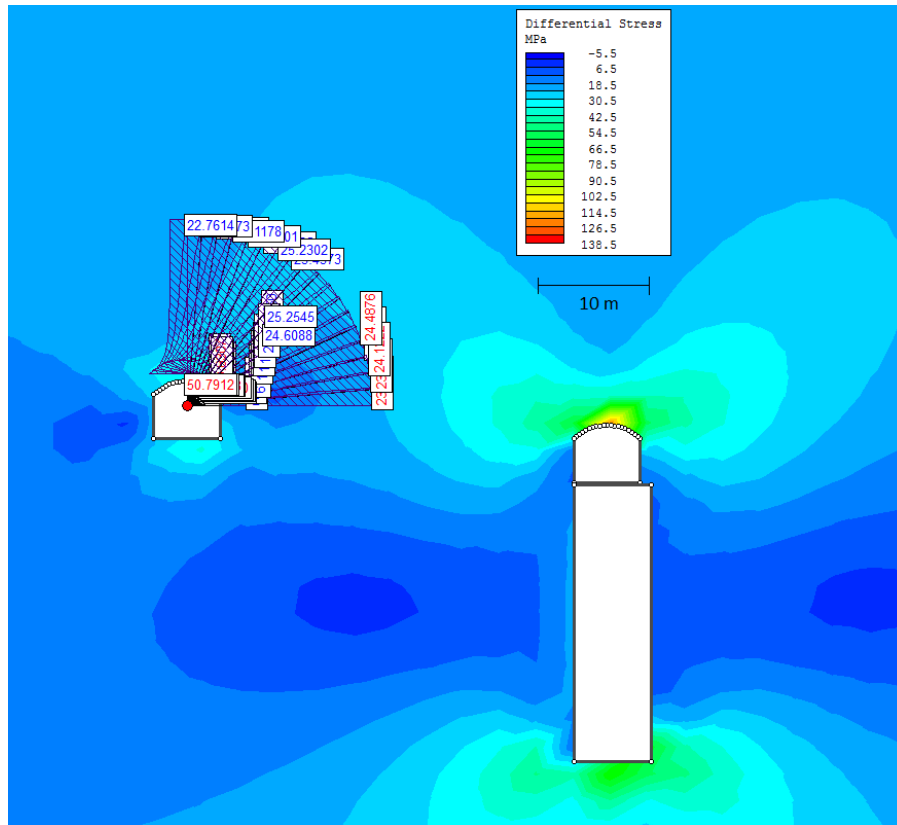


Figure 8. Modelled differential stresses before excavation of the stope.

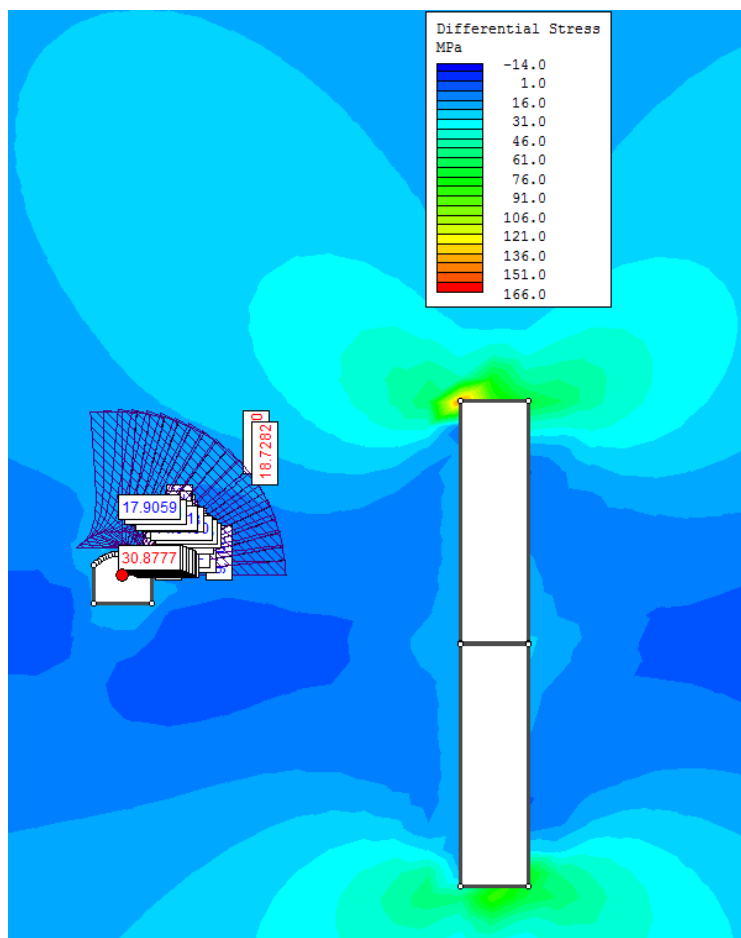


Figure 9. Modelled differential stresses after excavation of the stope



The second model presented in Figure 9 represents the situation after the stope has been excavated. As can be seen of the comparison of Figure 8 and Figure 9 the stress state changes due the excavation of the stope. In the measurement are there are also considerable principal stress direction changes.

First in the modelling the original total displacements caused by the earlier excavation were calculated. The displacements were calculated by deducting the minimum total displacement along the data query representing the extensometer from the maximum total displacement along the query. After this the total displacements after the studied excavation were calculated using the same method. By combining these two cases it was possible to calculate the total displacement caused by the excavation. The total displacement along the query was calculated. These calculations are shown in Appendix 1.

The results for the total displacements are shown in the Table 3. The chosen angles for the extensometers to be installed are presented with green marks.

**Table 3. Displacements before excavation of the target stope. The locations where extensometers were planned to install are on bold.**

<i>Angle of the query (Deg.)</i>	<i>Total Displacement (mm)</i>
0	1.3
5	1.1
10	0.4
15	0.6
<b>20</b>	<b>0.1</b>
25	0
30	-0.2
35	-0.5
40	-0.3
45	-0.5
<b>50</b>	<b>-0.6</b>
55	-0.6
60	-0.8
65	-0.7
<b>70</b>	<b>-0.8</b>
75	-0.9
80	-0.8
85	-0.9
90	-0.9

The modelled 3D case was more complex than the 2D model. The 3D model includes multiple stopes and one level. The data was gathered from database of the mine and sur-pac models created of the stopes were used to create the model. In total nine stopes and one level were included into the model.

The first step in the modelling was to gather all required stopes from the mines database. The stopes on the same level and above and under the level were decided to include into the model. As in the previous 2D model the backfilled stopes were decided to model as empty stopes since only marginal amount of stresses go through backfill due to its physical properties.

The second step of the modelling was to create a mesh using Rhinoceros 3D modelling software. The Surpac models were first converted into drawing exchange files (DXF) and then imported into Rhinoceros. In the Rhinoceros the files were first transferred into solids and it was checked that the solids were closed to enable the calculations.

After solids were confirmed to be closed each solid representing level or stope was converted into a mesh to enable the calculations in Examine3D. In the last step all the meshes touching each other were combined to prevent calculation errors with Examine3D which uses boundary element method.

The third step was to import the model created in Rhinoceros to Examine3D. The model is shown from two directions in Figure 10 a) from North and b) from East. The area to be mined is marked with red circle and the installation location is showed with blue arrow. In the beginning problems occurred such as that the Examine 3D could not use the data when the coordinates were in the coordinate system which the mine uses. This problem was solved by changing the center of the model to be in zero coordinate.

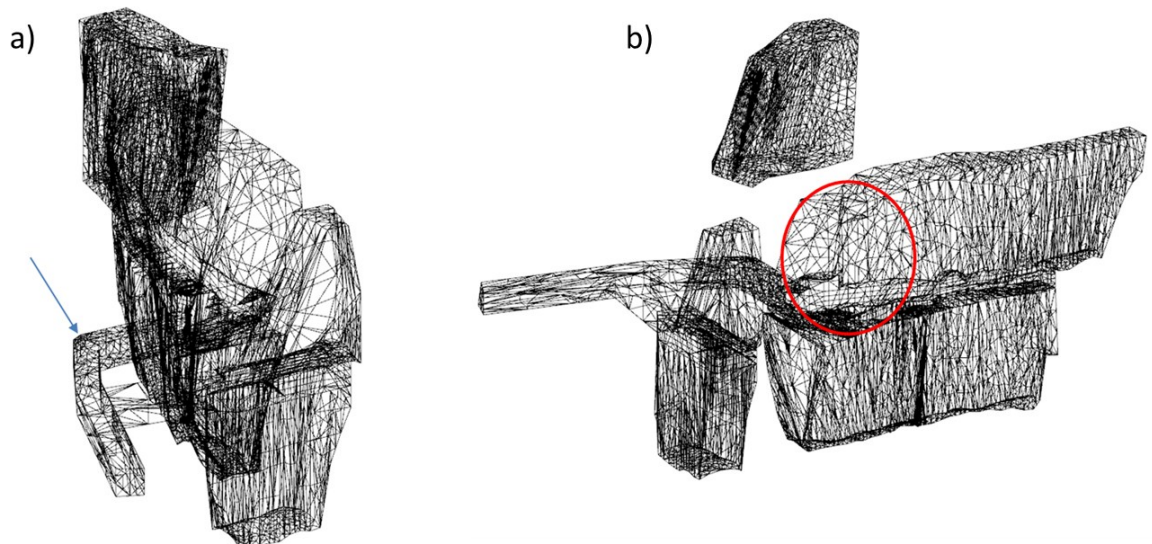


**Figure 10. Rhinoceros model of the level 410 test site. Excavation target marked with red and the measurement site with blue arrow. a) from North and b) from East.**

The used modelling parameters were the same as in 2D model and can be seen in Table 2. More realistic would have been to increase the stresses due to deeper location but since the mine has not done multiple stress measurements, the stress coefficient relative

to depth was unknown. Also, the purpose of the modelling was to find out the optimal locations for the extensometers and especially to confirm the directions of displacements.

### 3.3 *Experiment instrumentation*

For the later parts of the study it is essential to understand how the instruments measure the displacements and how the displacements can be converted into strains. It was equally important to ensure that the instruments were installed according to the manufacturer guidelines to avoid any errors caused by installation errors.

### 3.4 *Instruments*

The instruments used in this study were delivered by Mine Design Technologies Inc (later referred as MDT). The instrumentation of this study consists of 15 extensometers and four dataloggers.

The extensometers used were Smart MPBXs (Multi-Point Borehole eXtensometers) containing six anchor points each. For the purposes of the study a stroke of 127 mm was considered to be sufficient. Extensometers with two different lengths were used. The chosen lengths were 12 m and 20 m. The lengths were decided based on the distance from installation site to the target stope.

Because the extensometer has six anchor points it produces six different displacements along its length. Example of the extensometer is presented in Figure 11. Each of these displacements can be used as input data for the back calculation algorithm.

The extensometers can only measure strain. In case there was contraction the structure of the extensometer can prevent part of the movement (Dulmage 2015). This fact has to be considered when optimizing the locations of the extensometers. The contraction is prevented by the stiff structure of the extensometer.

Using of dataloggers was forced by the existing conditions because Kylylahti mine does not have wireless network to be used for wireless real time monitoring. Dataloggers were MDTs SmartLog3 dataloggers which are able to monitor up to three extensometers. The sampling rate can vary from one second to one day. In this study sampling rate of four hours was used. The dataloggers are battery-powered and the batteries can last up to two years depending on the sampling rate. (MDT brochure 2015)

The dataloggers and the handheld readout unit, which was also used for the measurements, measure voltage coming back from the extensometers. This way it can be found out how much the extensometer has extended or contracted. The system sends electric current into the extensometer when both current and voltage are known the electrical resistance can be calculated using the simple equation of Ohm's Law  $R = \frac{U}{I}$  where R is resistance, U is the potential difference and I the electric current.

The resistance is used to calculate the displacement of the extensometer. The displacements are used to calculate the strains for each extensometer within Smart units. The structure of the Smart MPBX is showed in Figure 11. The potentiometer of the extensometer is located at the head of the instrument.

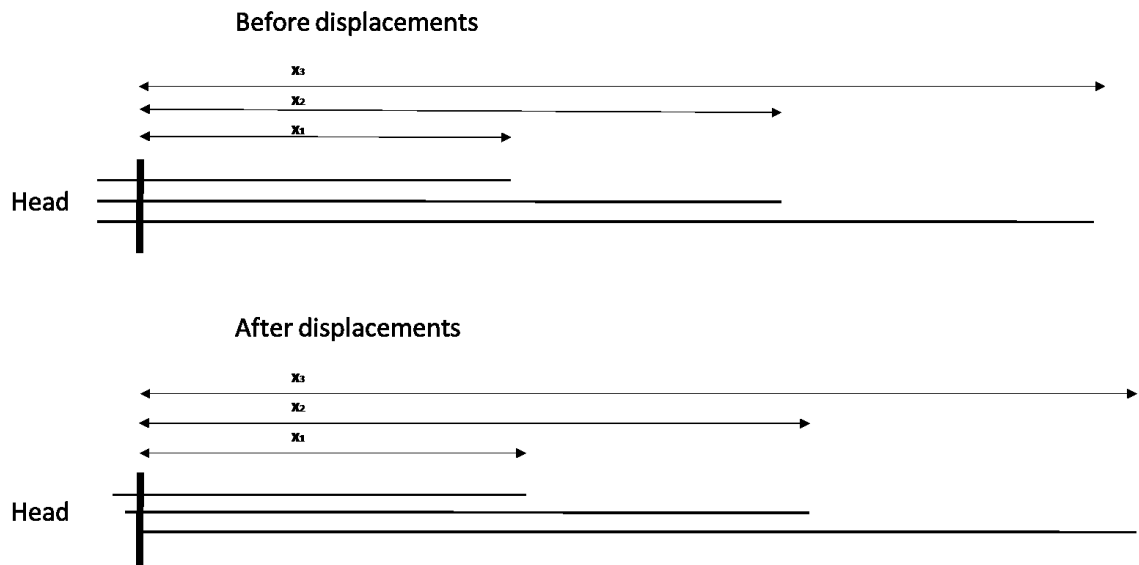


Figure 11. Structure of the SMART MPBX. (Tod J. & Lausch P.)

As can be seen from the Figure 11 each of the anchor points of the MPBX are connected to head of the instrument. In this study the instruments used had the head at the toe of the borehole. The structure of the extensometer impacts the modelling decisions made later in this study. Because of the structure of the instrument, the strains can be calculated as following  $\varepsilon = \frac{d^i - d^{i+1}}{L^{i+1} - L^i}$  where  $\varepsilon$  is the strain between two known points,  $L^i$  is the location of the instrument and  $d^i$  is the displacement in known location of the instrument.

There is also major difference between the handheld readout unit and the datalogger in accuracy. The Handheld readout unit can only measure in accuracy of 1 volt whereas the datalogger can measure in accuracy of up to 1/100 volt.

Typically these type of instruments are used for design verification and to monitor high risk areas where high displacement occur. Nowadays more used instrument type is cablebolt extensometer and it was also considered to be main instrument for this study. In the cablebolt extensometer the actual extensometer is build next or inside an cablebolt and it is measuring the extension of the cablebolt.

The MPBX was chosen over cablebolt extensometers due to the time table of the study. The cablebolt extensometers have to be installed at the same time as the normal cablebolts to ensure that they are included into the normal bolting pattern. If they are installed afterwards, the extra support gained from the cablebolt extensometer might affect to the results.

Example of how the MPBXs and cable extensometers are used can be seen in article by Bawden & Tod (2002). In this article the use of SMART instruments to verify support is described. The article also describes the MPBXs way of acting in more detail.

### 3.5 *Installation procedure*

The extensometers were installed using Ø 76 millimeter drillholes. The holes were drilled with Sandvik Solo longhole drilling machine. The holes were drilled slightly differently than the normal production holes. Lower feed pressures and new drill crown were used to decrease the possibility of deviation of the drillhole and to avoid drillhole blockages. Photos of the installation site and the drillholes are presented in Figure 12.



**Figure 12. Measurement site before installation of the extensometers**

The drillholes were visually inspected only from the start of the drillhole since there were no borehole cameras available.

The location and direction of the drillholes were measured as presented in the Figure 13. The measurement was done by inserting a Ø 76 mm drillrod into the drilled hole and measuring the end and starting point of the drill rod. The holes were measured to be in the right direction and at the planned location. The measurement errors caused by the



measurement technique were considered to be small. The technique is demonstrated in the Figure 13.



**Figure 13. Location and direction measurement of the drillhole**

The grouting of the extensometers was done with Sandvik Robolt bolting machine. The cement to water ratio was aimed to be 0.42 as the installation guide suggestion. The grouting of the extensometers was done using toe grouting. In toe grouting the grouting hose and the extensometers are inserted into the hole at the same time. When the grouting hose and the extensometer reach the end of the hole, pumping of the grout is started. The grouting hose is slowly pulled out from the hole. The goal is to keep the hose all the time in grout to ensure that the hole fully filled with grout.

The first installations were done at level 322 at the end of December. The goal was to install three extensometers as presented in Figure 14. The first two extensometers were installed without any significant problems but at the end of grouting the second extensometer the grouting hose split due to high pressure in the hose. Due to this reason the last extensometer was not installed. The extensometer which was not installed according to plan is presented in the figure as red.

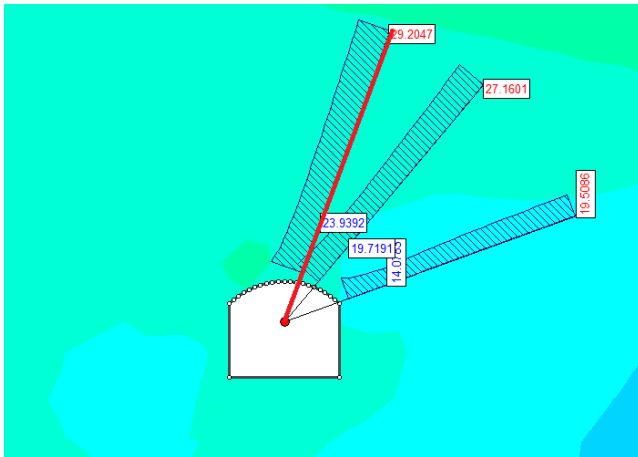


**Figure 14. Installed extensometers presented with Examine2D.**

The second installation was done at level 410 at middle of January. The goal was to install 11 extensometers. The configuration of the extensometers is shown in Figure 15. The installation took in total 12 hours.

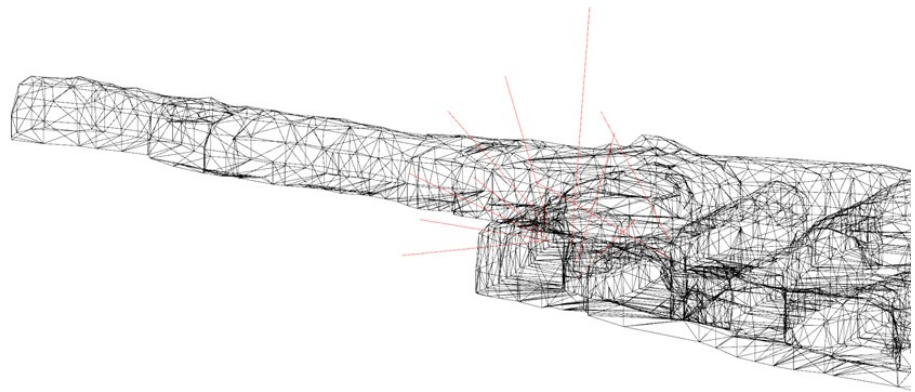


**Figure 15. Locations of the extensometers at level 420**

## 4 Verification of the back calculation method

In this chapter the algorithm presented in chapter 2 is tested using synthetic data created with Examine 2D. This was done to ensure that the modelling selections done for this study were adequate for the algorithm to be used.

Approach of conducting simple analysis first and then moving for more complicated analysis was decided to be used. The chosen steps to be done were simple 2D analysis with synthetic data, synthetic 2D data with shear stress analysis and finally the 2D data analysis with shear stress analysis. The synthetic data test without shear stress were left out from this study but results were similar to results gained with shear stress component.

### 4.1 *Synthetic 2D analysis*

The algorithm and the Matlab code written were only used with synthetic data created with Examine2D and Comsol. To ensure that the code works well with similar data that the extensometers produce, it was tested first with synthetic data. The method to create synthetic data was changed to produce similar data as the real extensometer.

The first task was to simulate extensometers using Examine2D and to form load cases from these simulation. The load cases were formed by adding unit loads for each  $\sigma_x$ ,  $\sigma_y$  and  $\tau_{xy}$ . Forming of the load cases is shown in Figure 16. In the modelling the unit load was chosen to be 100 MPa instead of 1 MPa to enable more precise data handling with MatLab.

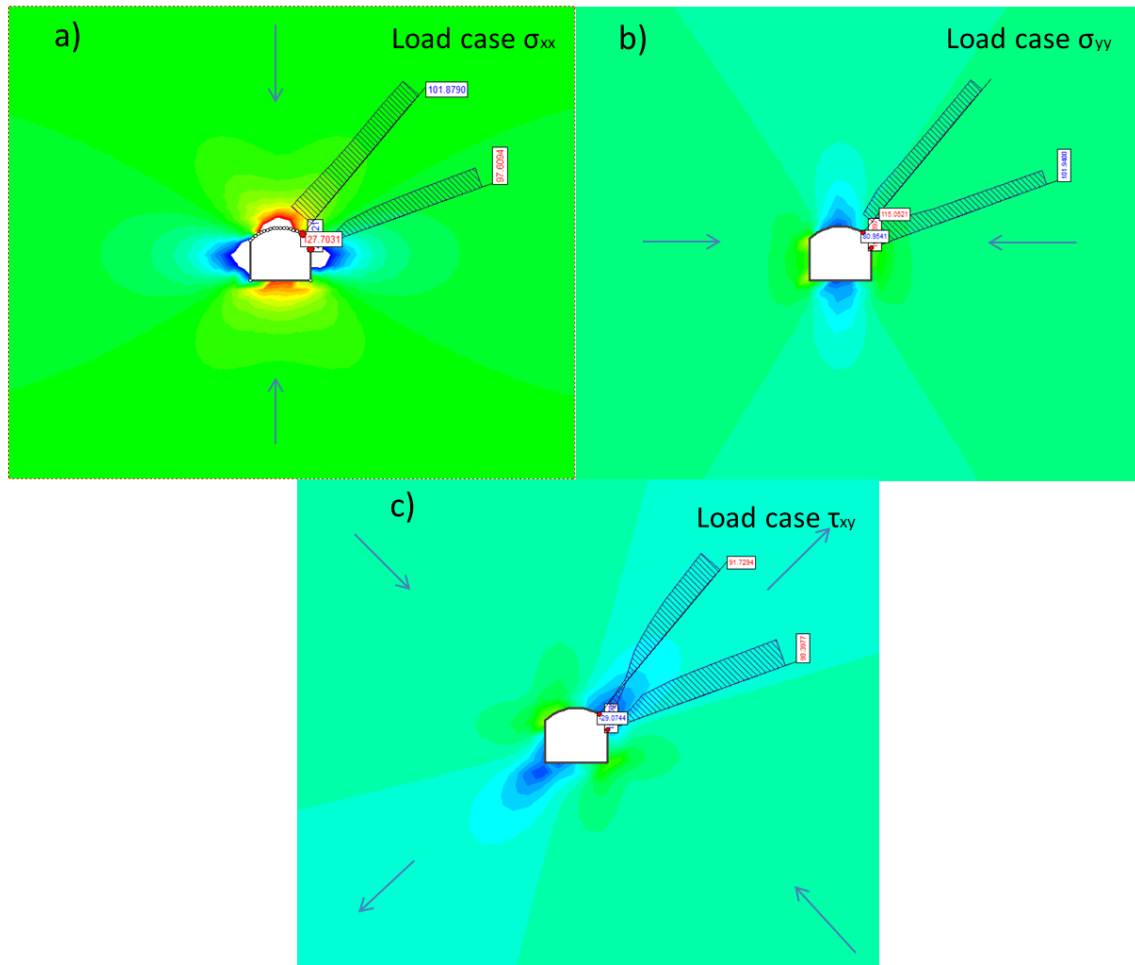


**Figure 16. Forming method of the load cases. a) Load case  $\sigma_{xx}$ , b) load case  $\sigma_{yy}$  and c) load case  $\tau_{xy}$ .**

The shear ( $\tau_{xy}$ ) load case was formed by placing unit loads for both  $\sigma_x$  and  $\sigma_y$  with  $\sigma_y$  being -100 MPa and the angle between the unit loads to be  $90^\circ$ . With this combination the mean stress decreases to zero. The combination is explained in Figure 17.

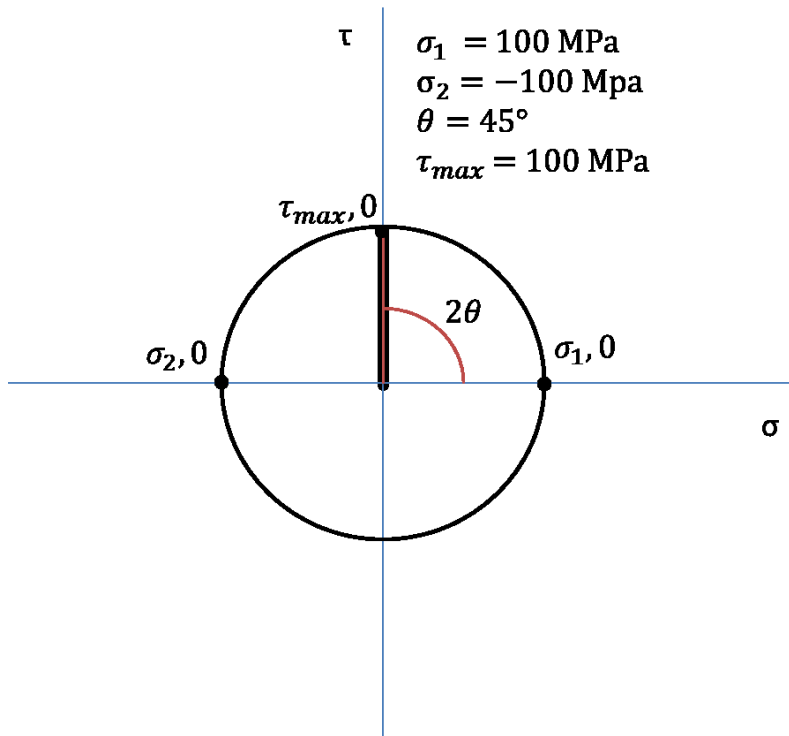


Figure 17. Mohr's circle example of shear stress load case.

The amount of load cases is dependable on the amount of variables to be solved. In two-dimensional case there are three variable to be solved as can be seen from the equation 4.

$$S = \begin{bmatrix} \sigma_x & \tau_{xy} \\ \tau_{yx} & \sigma_y \end{bmatrix} \quad (4)$$

The strains were calculated from the model using displacements. The calculation method is showed in Table 4. First the total length of the extensometer before the excavation was calculated. After this the total length of the extensometer after the excavation was calculated. The final step was to calculate the strain by subtracting the old length from the new length and then dividing the result with the old length.

**Table 4. Strain calculations from the Examine2D model. Y1, Y2, X1 and X2 are coordinates of the extenometer.**

	<i>New</i> <i>X1</i>	<i>New X2</i>	<i>New</i> <i>Y1</i>	<i>New Y2</i>	<i>New length</i> <i>(m)</i>	<i>Previous</i> <i>length (m)</i>	<i>Strain</i>
<i>0 to 3.33</i>	7.05	8.83	6.72	8.85	2.78	2.78	-1.74E-04
<i>0 to 6.67</i>	7.05	10.61	6.72	10.98	5.55	5.56	-3.00E-04
<i>0 to 10</i>	7.05	12.39	6.72	13.11	8.33	8.33	-4.00E-04
<i>0 to 13.33</i>	7.05	14.17	6.72	15.24	11.11	11.11	-4.84E-04
<i>0 to 16.67</i>	7.05	15.95	6.72	17.37	13.88	13.89	-5.58E-04
<i>0 to 20</i>	7.05	17.73	6.72	19.50	16.66	16.67	-6.20E-04

For the synthetic case same modelling parameters were used as in pre-modelling phase. These parameters can be found in Table 2. The following stress state was chosen to be modelled:

$$\sigma_1 = 10 \text{ MPa}$$

$$\sigma_2 = 5 \text{ MPa}$$

$$\sigma_z = 0 \text{ MPa}$$

$$\text{Angle} = 0^\circ$$

The back calculation results of the synthetic data were as following:

$$\sigma_1 = -9.89 \text{ MPa}$$

$$\sigma_2 = -4.82 \text{ MPa}$$

$$\tau_{xy} = -0.09 \text{ MPa}$$

These results were considered to be accurate enough to continue with next step of the algorithm verification. The error between modelled and simulated stresses were as following:

$$\text{Error}_{\sigma_1} = 1.1 \%$$

$$\text{Error}_{\sigma_2} = 3.6 \%$$

## 4.2 2D synthetic analysis with near field modelling

The second round of the synthetic data analysis was to try the impact of the near field analysis to the results obtained from the method. In the near field analysis also tunnels and structures near the tunnel are included into the model. The modelled area is shown in Figure 18.

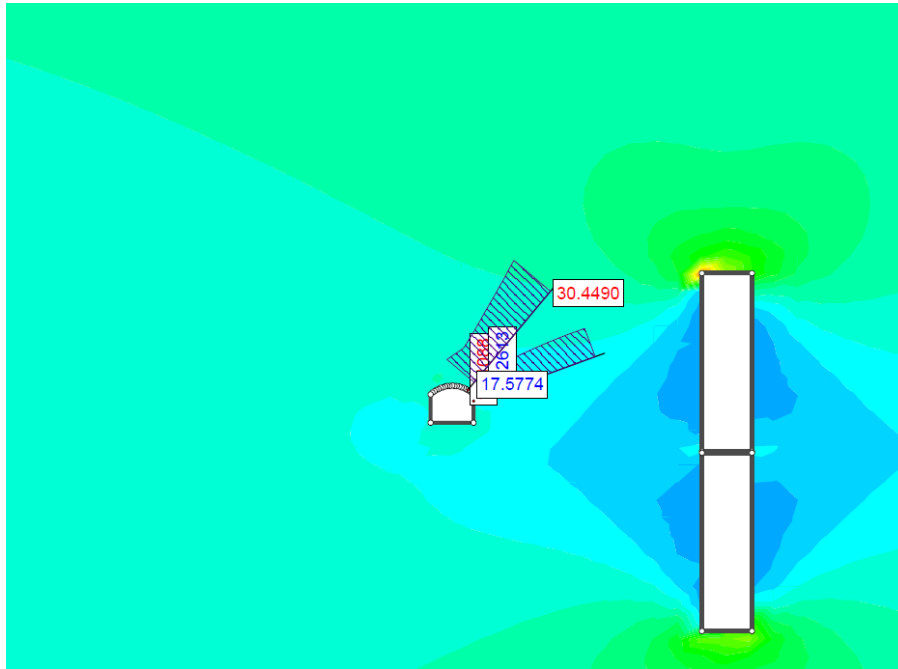


Figure 18: Example of the near field model.

Again the same parameters were used as in pre-modelling phase (Table 2). The following stress state was chosen to be modelled:

$$\sigma_1 = 30 \text{ MPa}$$

$$\sigma_2 = 10 \text{ MPa}$$

$$\sigma_z = 0 \text{ MPa}$$

$$\text{Angle} = 0^\circ$$

The back-calculation results of the synthetic data were as following:

$$\sigma_1 = 30.01 \text{ MPa}$$

$$\sigma_2 = 10.12 \text{ MPa}$$

$$\tau_{xy} = -0.02 \text{ MPa}$$

The errors were following:

$$Error_{\sigma_1} = 0.33 \%$$

$$Error_{\sigma_2} = 1.2 \%$$

As can be noted the error from the near field analysis was minimal and smaller than with far field analysis. This can be explained with greater strains modelled in the near field analysis.

### 4.3 **2D synthetic analysis with shear stress**

In the last two dimensional synthetic analysis an angle between the  $\sigma_1$  and  $\sigma_2$  was introduced. This was done to verify that the final part of the algorithm works. The final part of the algorithm solves the angle between the two main stresses using  $\sigma_1$ ,  $\sigma_2$  and  $\tau_{xy}$ .

The parameters used for the modelling were same as previously. The modelled stress state was following:

$$\sigma_1 = 10 \text{ MPa}$$

$$\sigma_2 = 5 \text{ MPa}$$

$$\sigma_z = 0 \text{ MPa}$$

$$Angle = 15^\circ$$

Prior to Cauchy equations algorithm produced following results:

$$\sigma_{xx} = 7.49 \text{ MPa}$$

$$\sigma_{yy} = 7.49 \text{ MPa}$$

$$\tau_{xy} = 2.49 \text{ MPa}$$

Using the final part following results were obtained:



$$\sigma_1 = 9.98 \text{ MPa}$$

$$\sigma_2 = 5.01 \text{ MPa}$$

$$\text{Angle} = 15.03^\circ$$

The errors in the synthetic case were following:

$$\text{Error}_{\sigma_1} = 0.22 \%$$

$$\text{Error}_{\sigma_2} = 0.15 \%$$

$$\text{Error}_{\text{angle}} = 0.01 \%$$

Figure 19 shows the fit between synthetically created “measured” data and the modelled data. The two extensometers are marked with different colors. As can be seen from the figure, the correlation between the modelled and synthetically created measured data is high and the data fits well to the regression line. Also the results obtained from the case were excellent due to a really small errors.

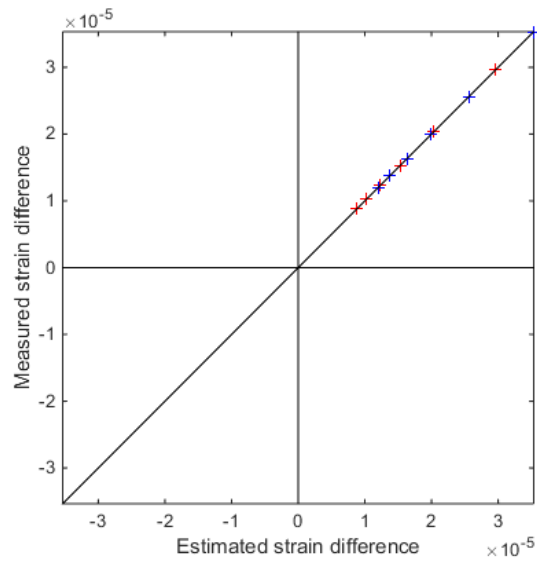


**Figure 19. Estimated strain difference against "measured" strain difference with synthetic data.**

## 5 Monitoring and back calculation results

### 5.1 Executed excavations

In Kylylahti mine Sublevel stoping with backfilling is used. The direction of the stoping varies by the thickness of the ore. Both stopes monitored in this study are at the narrow part of the orebody where sublevel stoping is used in conventional way. On the level 410 also the stopes over and behind the target stope are mined using sublevel stoping in conventional way.

In this study two different excavations were monitored. The first monitored excavation was on level 325 at depth of approximately 420m. The excavation geometry was simple and it is presented in Figure 7. The total excavated volume was approximately 8000 m<sup>3</sup>. The excavation of the stope started at the end of December 2014 and ended at the middle of January 2015. The backfilling of the stope started in February.

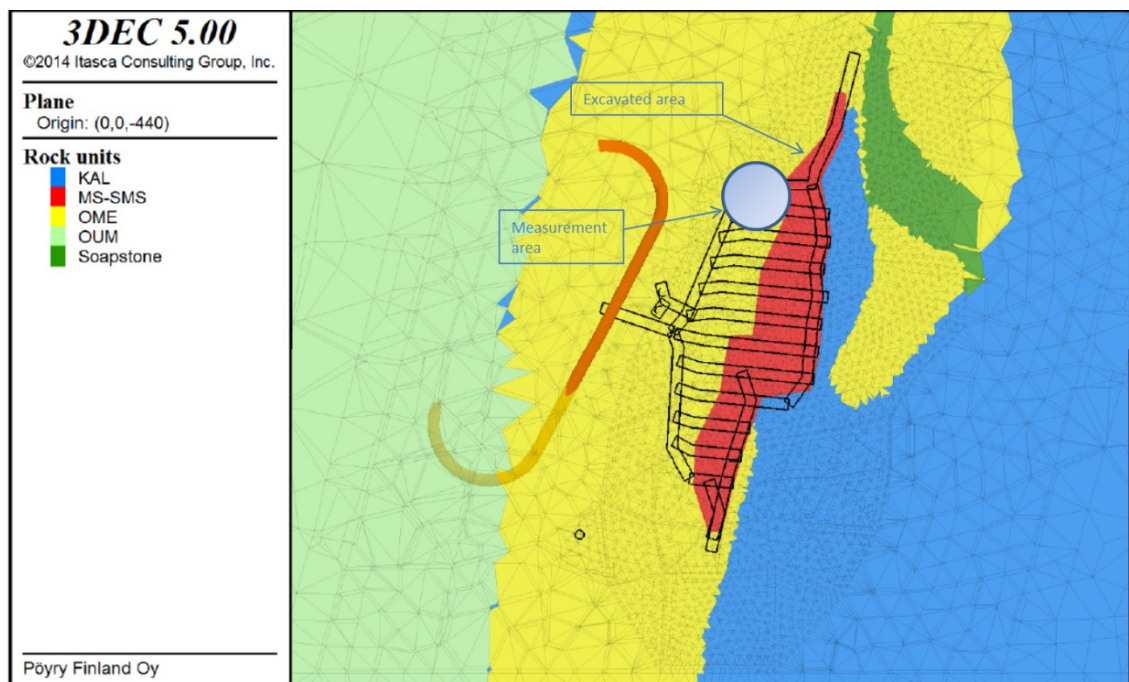


Figure 20. Rock units under the excavated area. 3DEC model. (Picture given by Boliden Kylylahti)

The second excavation was located at level 410 at depth of approximately 500m. The geometry of the level is more complicated than at the first excavation. The geometry is shown in Figure 20. On the west side of the stope there is soap stone zone. Some mining had already been done at the level and at the levels on and under. The mined stopes and the 3D geometry of the level are shown in Figure 10.

Notable is that near the stope, which is the main interest of the study, mining had already started. Stopes both behind and on top of the stope in interest were already mined. Some stress state change had already occurred and there were signs of stress state change at the level in form of onion peeling of one of the pillars near the excavated stope.

The stope was chosen to be target of the study because it had the least impacted surroundings of the stopes to be mined within the time frame of the study. The best solution for a monitoring site would have been an unmined virgin level but this was not possible due the time frame of the study.

The total volume excavated from the stope was approximately 37 000 m<sup>3</sup>. The stope was mined using heavy sequencing and the stope was mined with total of 13 blasts of which eight were production blasts. The sequencing is shown in Figure 21. In total the stope was in production for one month. The biggest blast was shot on 14<sup>th</sup> of February.

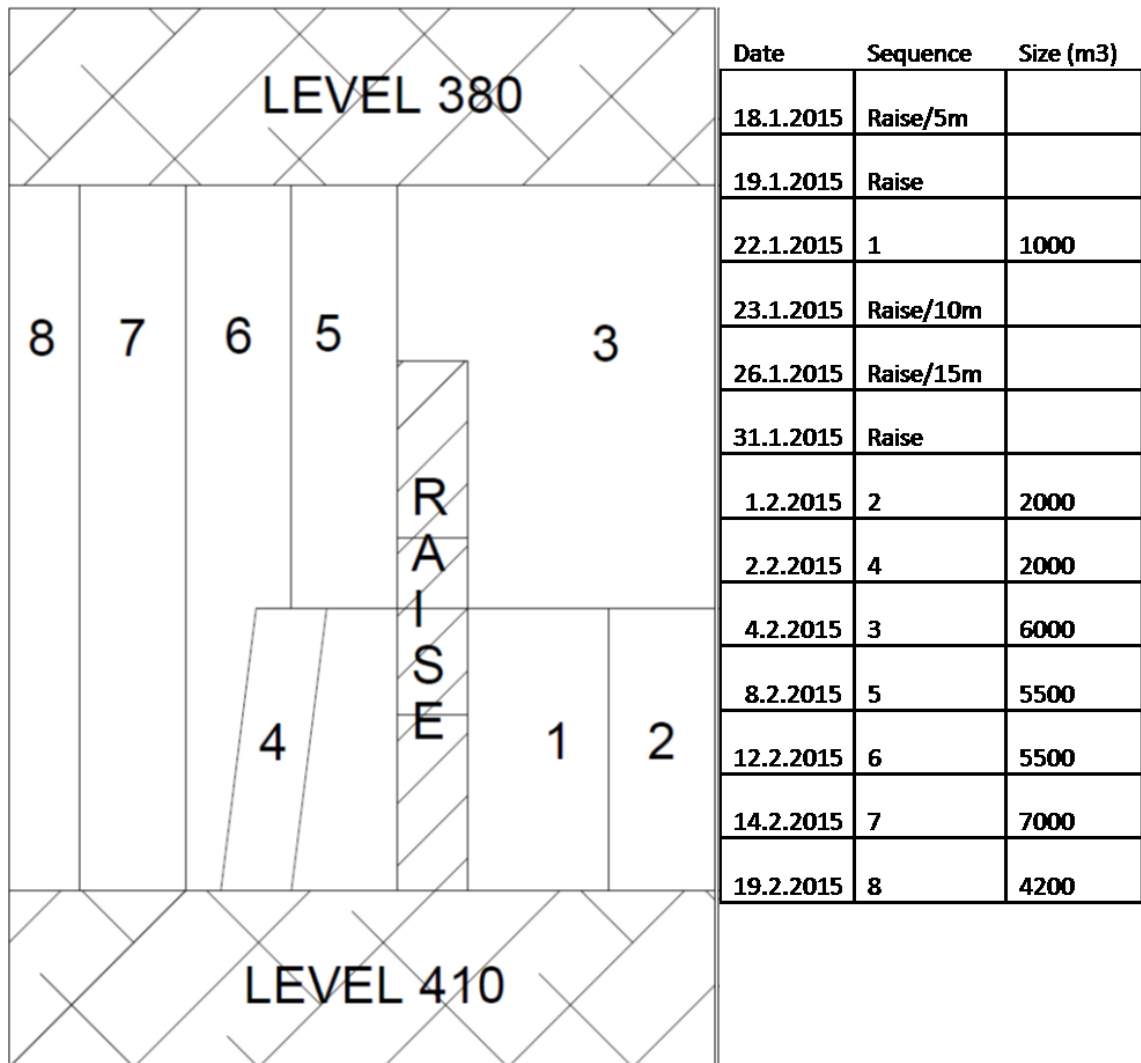


Figure 21. Target excavation on level 410 sequenced mining and dates from 2D perspective.

## 5.2 Rock mass response of 2D test site

The rock mass response of both sites was done prior of analyzing the data with the inversion code developed in the Dynamine project. This was done to see if there were any irregularities or sources of errors in the data.

At the first test site it was noted that the handheld readout unit and the datalogger did not give entirely same readings. This caused discontinuity to the measurements. When this was noticed a decision was made to use only handheld readout unit. Using the only data gathered with dataloggers was impossible due to lack of proper comparison point and due to short measurement period which did not include all the excavation phases.

In total at the first test site most of the deformations could be classified as elastic deformations because of the magnitude of the displacements. Example of strains calculated from the extensometer measurements are shown in Figure 22. The particular extensometer was located at level 325 at Kylylahti Mine and it was installed into angle of 20 degrees (Figure 22). The other extensometer located at the test site gave similar results compared to the one shown in Figure 22.

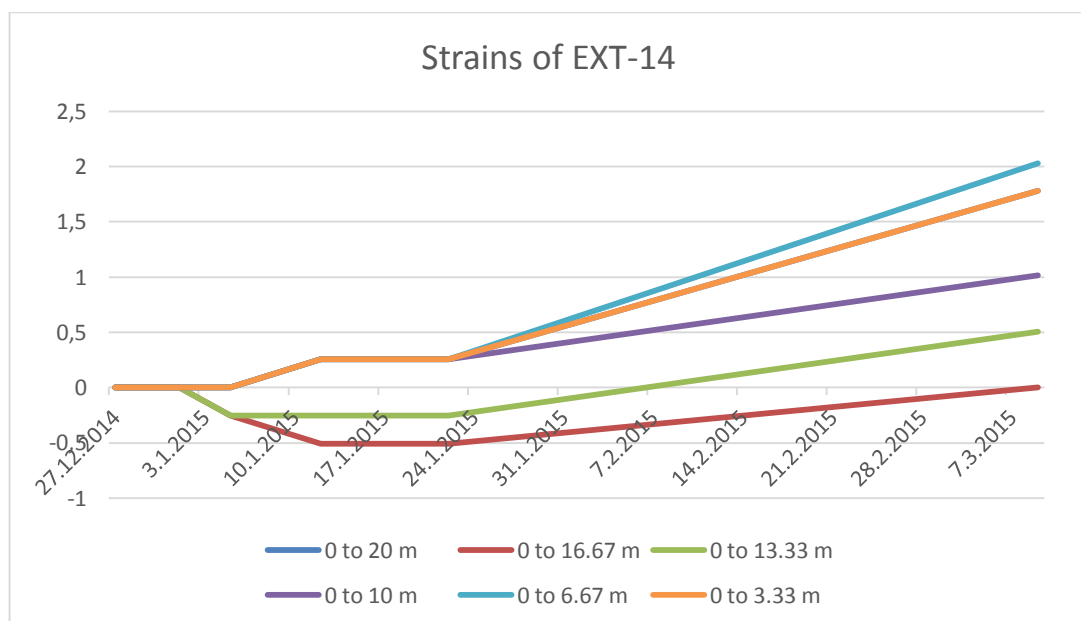


Figure 22. Strains of EXT-14 located at the test site 1.

The rock mass response at level 325 was as expected by the simulations. It was noted that part of the displacements were measured as late as 9<sup>th</sup> of March, nearly two months after the initial excavation. These displacements were considered to be caused by the continuation of the excavation at the level. The next stope on the level was located so that it supported and extended the 2D geometry and increased the plain-strain conditions.

There is also clear trend visible in the measured strains. This trend indicates that the data gathered is useful for the analysis with the 2D algorithm.

### 5.3 ***Rock mass response of 3D test site***

The results from the second test site were not as expected from the simulations. There were considerable amount of deformations that are interpreted to be plastic due to their magnitude. There were also extensometers where the trend of displacement was towards contraction instead of strain.

During the monitoring period one of the extensometers was lost due a fly rock from the excavation. The data gathered from this extensometer was excluded from further analysis.

The monitoring results gave also high displacements, over 10 mm, at many locations. These displacements were thought to be caused by opening of joints because of their magnitude.

It was also spotted that the displacements measured from the test site two were considerably higher than the results from the first test site. There were also more readings that were not useful for the study because of their magnitude.

The rock mass at the test site two was probably more disturbed than the rock mass at the first test site. In the level 410 and in the levels above and under it mining had already started and this probably impacted to the results gained from the measurements. Also the level had visible stress related damage in form of onion skinning of the pillars. During the excavation of the stope hard noises from the rock mass was heard. This indicates high stress release.

The onion skinning and other stress related damage may have affected the measurements in a way that it highly impacts to the results gained from the algorithm.



#### 5.4 *Preparation of the data*

The data gathered from the Kylylahti mine was received at March 2015. The first task was to check the sufficiency of the data quickly. During the data check it was spotted that the data included noise which was larger than expected. The example of the degree of the noise is show in Figure 23.

Some of the strain measurements also showed that there were plastic deformations which most probably were caused by opening and closing of the joints near the excavated areas. The data of one of the extensometers which shows clear plastic deformation is shown in Figure 23.

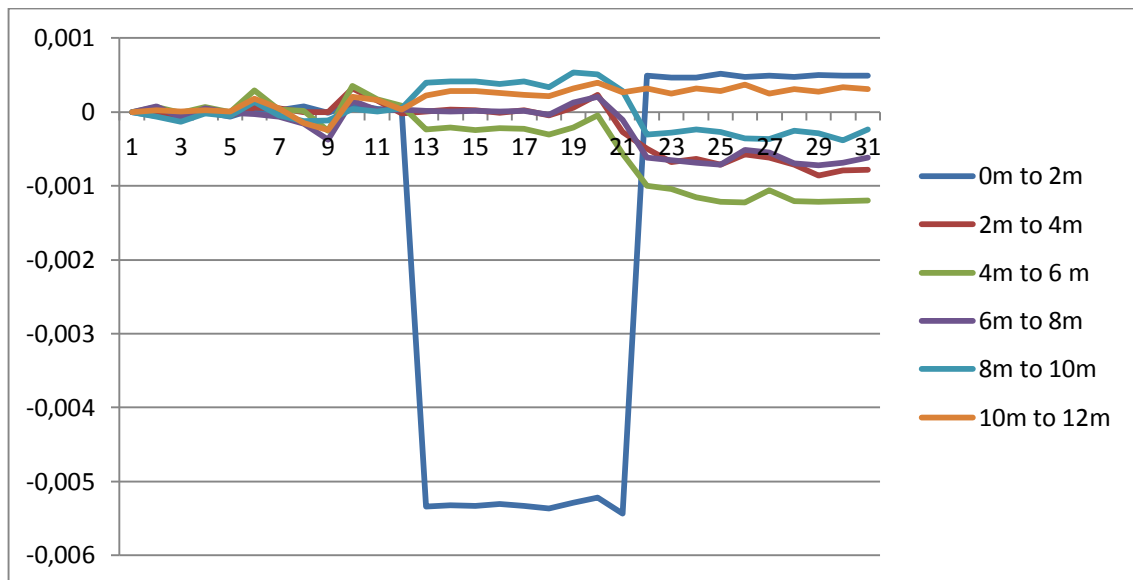


**Figure 23. Plastic deformation example (0 to 2m).**

The data for 2D was gathered manually and with datalogger. The data provided manually and with datalogger differed by a scale that was meaningful for the study. The error regularity was tested but no constant error term was found. At this phase it was decided that the manual data and data gathered with datalogger were to be processed separately and the main concentration of interest would be in manually collected data due to the fact that it was available from longer time period.

The 3D data was gathered only with dataloggers. The dataloggers were set to measure the extensometers every four hour. Due the purpose of the study and to avoid errors

caused by the activities in mine only one measurement per day was included into the processed data. Example of the used data is provided in Table 5.

**Table 5. Example data set of measured displacements from the Kylylahti.**

<i>Reading Date</i>	<i>12.00m</i>	<i>2.00m</i>	<i>4.00m</i>	<i>6.00m</i>	<i>8.00m</i>	<i>10.00m</i>
<i>2/21/2015</i> <i>5:56:04 AM</i>	112.281	67.76	2.555	6.149	121.615	60.843
<i>2/20/2015</i> <i>9:56:04 AM</i>	106.017	64.392	6.49	8.715	115.151	58.014
<i>2/19/2015</i> <i>9:56:04 AM</i>	-1.295	3.559	1.702	-	8.064	-
<i>2/18/2015</i> <i>11:51:45 AM</i>	7.17	1.019	-0.508	-	-11.524	-15.86
<i>2/17/2015</i> <i>11:51:45 AM</i>	-0.178	-0.051	0.14	-0.391	-0.051	-0.241
<i>2/16/2015</i> <i>11:51:45 AM</i>	-0.224	-0.168	-0.234	-0.363	-0.236	-0.241
<i>2/15/2015</i> <i>11:51:45 AM</i>	-0.157	-0.094	-0.188	-0.249	-0.17	-0.135
<i>2/14/2015</i> <i>11:51:45 AM</i>	-0.178	-0.114	-0.368	-0.531	-0.391	-0.439
<i>2/13/2015</i> <i>11:51:45 AM</i>	-0.173	-0.185	-0.33	-0.264	-0.287	-0.198

### 5.5 2D analysis with far field modelling

After the data was simplified to be suitable for the analysis the algorithm used for the analysis was tested with synthetic data. New synthetic data test were done to ensure that the algorithm was fully functional and able to intake the data in a format which it was gathered.

As described previously for the 2D analysis only the data gathered manually was to be used in 2D analysis. Example of data used is shown in Table 6. The measured data is presented as strains in the table. The load cases used in the analysis were same as with the synthetic data analysis.

**Table 6. Strains from the 2D test site at the Kylylahti mine. Extensometer EXT-14.**

	<i>0 to 3.33</i>	<i>0 to 6.67</i>	<i>0 to 10</i>	<i>0 to 13.33</i>	<i>0 to 16.67</i>	<i>0 to 20</i>
<i>27.12.2014</i>	0	0	0	0	0	0
<i>31.12.2014</i>	0	0	0	0	0	0
<i>1.1.2015</i>	0	0	0	0	0	0
<i>5.1.2015</i>	0	0	0	0	-1.524E-05	-1.270E-05
<i>12.1.2015</i>	7.621E-05	3.810E-05	2.540E-05	1.905E-05	-1.524E-05	-2.540E-05
<i>22.1.2015</i>	7.621E-05	3.810E-05	2.540E-05	1.905E-05	-1.524E-05	-2.540E-05
<i>9.3.2015</i>	5.335E-04	2.667E-04	2.032E-04	7.620E-05	3.048E-05	0

In the first phase the back-calculation was done with both extensometers without outlier elimination. Both extensometers were processed at the same time. It was later noted the two extensometers did not produce similar results and thus gave bad results from the multiple linear regression.

The changes in the beginning of the measurement period were small and barely within the region of the measurement accuracy. After the second stope at the level 322 was mined the displacement and thus the strains increased. Mining of the second stope strengthened the two dimensional model by increasing the plain strain conditions.

**Table 7. Multiple linear regression multipliers obtained from the Kylylahti Mine data.**

	<i>Beta1</i>	<i>Beta2</i>	<i>Beta3</i>
27.12.2014	0	0	0
31.12.2014	-14.6578	-30.7194	7.1194
1.1.2015	-14.6578	-30.7194	7.1194
5.1.2015	-2.2333	-10.0077	-0.4445
12.1.2015	74.6452	108.5789	-41.2722
22.1.2015	67.1072	98.0126	-36.5784
9.3.2015	492.1425	726.088	-263.538

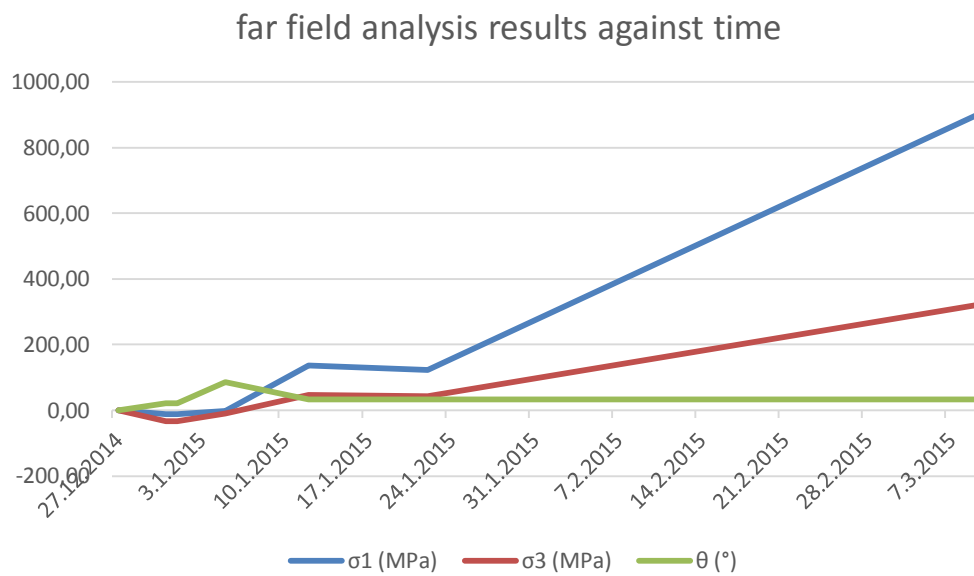
The beta factors gained from far field analysis are shown in Table 7. Already the beta factors showed that the results were poor. With small displacements at the beginning of the measurement period the algorithm gives results that are close being in the right magnitude but the fit between the estimated strain difference and the measured strain difference is poor due to the measurements having zero displacements were included in the data.

After the beta factors were calculated the results were transformed into principal stresses. These results are shown in Table 8.

When both of the extensometers start to record strains at 12<sup>th</sup> of January the results gained from the algorithm start to be in totally wrong magnitude. Also the fit in the linear regression is not perfect but improves from the earlier results. Example of typical fit is shown in Figure 26. In the figure it is obvious that the two extensometers have different fit with multiple linear regression. In the last measured data on 9.3.2015 the fit (Figure 25) between the two extensometers is excellent but the results are in totally wrong magnitude. The right magnitude in this case is in tens of MPas. This was derived from the preliminary modelling.

**Table 8. Final results of the far field analysis of the Kylylahti mine data**

	$\sigma_1$ (MPa)	$\sigma_3$ (MPa)	$\vartheta$ (°)
27.12.2014	0.00	0.00	0.00
31.12.2014	-11.96	-33.42	20.78
1.1.2015	-11.96	-33.42	20.78
5.1.2015	-2.21	-10.03	86.74
12.1.2015	136.24	46.99	33.83
22.1.2015	122.27	42.85	33.55
9.3.2015	897.45	320.78	33.03

**Figure 24. Plot of the results of the 2D far field analysis at the Kylylahti mine against time. Stresses in MPa and angle in degrees.**

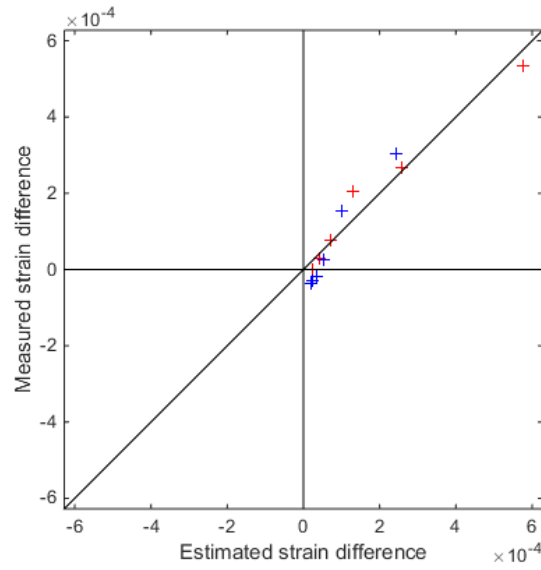


**Figure 25. Estimated strain difference versus measured strain difference. 9.3.2015. Extensometers marked with different colors.**

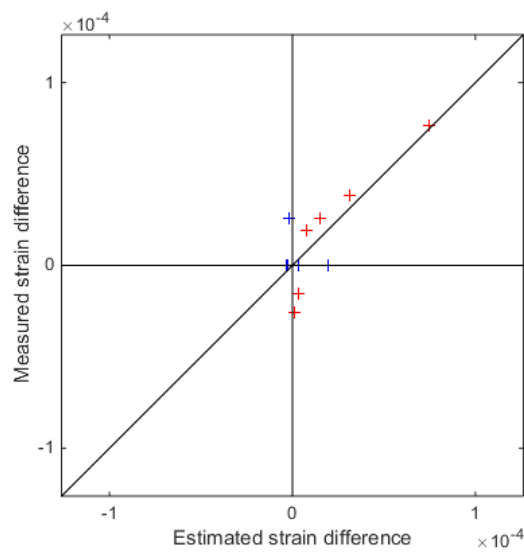


**Figure 26. Estimated strain difference versus measured strain difference. 22.1.2015. Extensometers marked with different colors.**

In total, the results gained from the far field analysis were not satisfying. The reasons affecting to the results are covered in chapter 6.

## 5.6 2D analysis with near field modelling

The data gathered from the Kylylahti mine was also processed with near field method. This was done because the distance from the mined stope to the test site was only approximately 30 meters. It was thought that this would cause change in the principal stress directions. This will change the modelled displacements.

The used near field model is shown in Figure 18 in chapter 4.2. Non-sequenced model was used in the first phase of the near field modelling. It was decided that the sequenced model would be only needed if the results gained from the 2D near field modelling would be in the right magnitude. Also in this point of the study outlier elimination was not used due to reasons mentioned previously.

The results of the near field analysis were better than from the far field analysis. The beta factors gained from the algorithm are shown in Table 9 and the final results in Table 10. At this point it was clear that stope was so close that the near field analysis were needed. The beta factors were in right magnitude except for the last measurement when the  $\tau_{xy}$  (or Beta3 factor) increased to higher level. The increase of the factor resulted to bigger changes in the final results for all the variables.

**Table 9. Multiple linear regression results of the Kylylahti mine data for the near field analysis.**

	<i>Beta1</i>	<i>Beta2</i>	<i>Beta3</i>
27.12.2014	0	0	0
31.12.2014	-2.2718	-15.703	0.0511
1.1.2015	-2.2718	-15.703	0.0511
5.1.2015	-3.3094	-18.2498	1.4486
12.1.2015	-2.3857	-14.3656	10.9688
22.1.2015	-2.6018	-13.4286	11.9085
9.3.2015	6.8345	-6.3141	53.8849

The final results gained from the last part of the algorithm were in satisfactory region except for the last measurement except for the final result gained from 9.3.2015 measurement. The signs of the first three results (31.12. – 5.1.) can be thought to be gained from noise of the measurements. From 12.1.2015 on the rock mass has started to behave more as expected.

The fits between the measured and estimated strains were similar as with the far field analysis. These fits from two days are shown in Figure 28 and Figure 29. Again as the strains increased the fits improved and the fit on 9<sup>th</sup> of March is already looking fairly similar as the fits with synthetic data.

It has to be noted that the multiple linear regression forms 3D surface in 4D space in this case with three variables and fitting the last parameters to the surface causes greater error than fitting the first parameters.

**Table 10. Final results of the near field analysis.**

	$\sigma 1$ (MPa)	$\sigma 3$ (MPa)	$\theta$ (°)
27.12.2014	0	0	0
31.12.2014	-2.2716	-15.7032	0.2181
1.1.2015	-2.2716	-15.7032	0.2181
5.1.2015	-3.1702	-18.389	5.487
12.1.2015	4.1221	-20.8734	30.6807
22.1.2015	5.066	-21.0964	32.7771
9.3.2015	54.5447	-54.0243	41.522



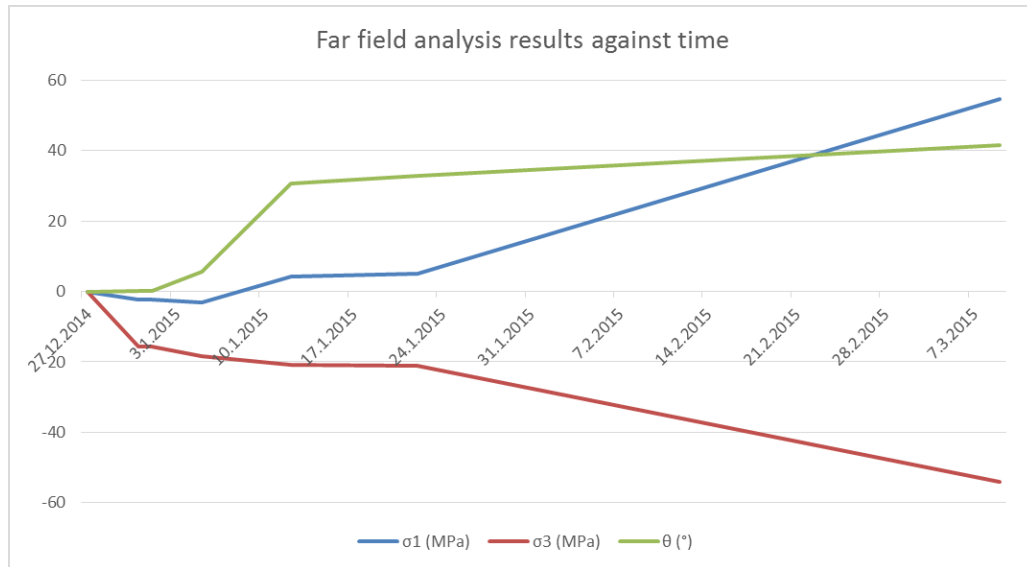


Figure 27. Near field analysis results against time.

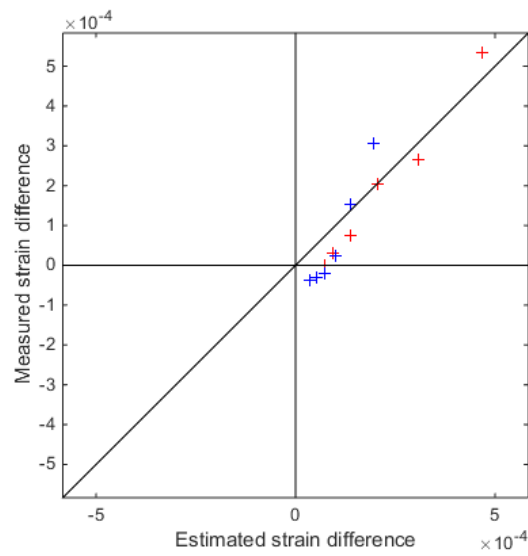
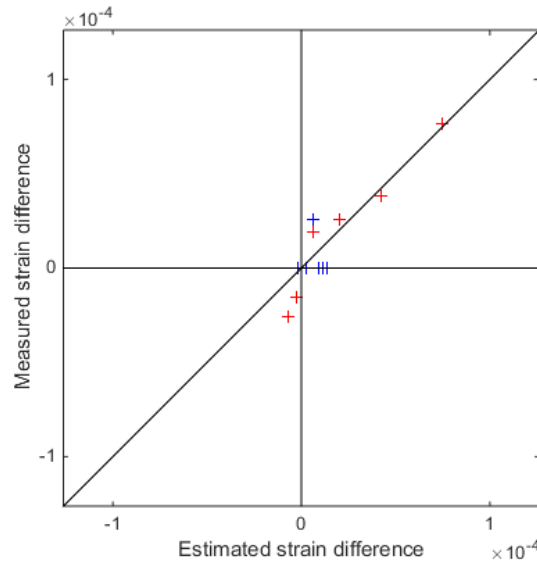


Figure 28. Measured strain 9<sup>th</sup> of March versus estimated strain with near field analysis. Extensometers marked with different colors.



**Figure 29. Measured strain 22<sup>nd</sup> of January versus estimated strain with near field analysis. Extensometers marked with different colors.**

In total, the results from the near field analysis were more satisfactory than the results gained from the far field analysis. The fits between the measured and estimated strain difference were good and the results except for the last measurement were in the right magnitude. Similar sources of error as in the far field analysis are still in the data set.

### 5.7 *2D near field analysis of the Posiva 2011 test site*

Because of the poor results obtained from the Kylylahti test site it was decided that already tested data would be more beneficial to be analyzed than new data with uncertainties. Main concern with the Kylylahti data was that the rock mass was more heavily previously disturbed in the 3D test than at the 2D test site.

A data set from Posiva was received for further testing of the algorithm. This data set was collected during excavation of new cavern next to an existing tunnel. The 2D geometry is shown Figure 31. The change caused by the excavation was measured accurately and it was in a region that was sufficient for the code, both extensometers showing displacements of over one millimeter. Also the rock type at the Posiva ONKALO test site was more suitable for the elastic analysis because it is more homogenous than the rock types affiliated with the Kylylahti mine measurements.

The measurement equipment was also different than used at the Kylylahti mine site. In ONKALO mechanical rod extensometers with electronic readout head were used.

Time frame of interest is shown in Figure 30 and it is marked with blue square. This time frame was chosen because it includes the major displacements at the test site and thus major stress changes.

The data collected from the test site was extensive and at the beginning of the test period data was collected every minute and after few days every hour. The amount of data was considered to be useless for the purpose of the study and thus data points were picked manually. The picked data points represent measurements when the major changes in the displacements occurred. The picked data points are shown in Table 11. The picked data was recorded at the same time. This was done to avoid unwanted sources of errors such as temperature differences.

The maximum measured displacements in the Posiva data were over two millimeters. The maximum displacements were reached at the end of November 2011.

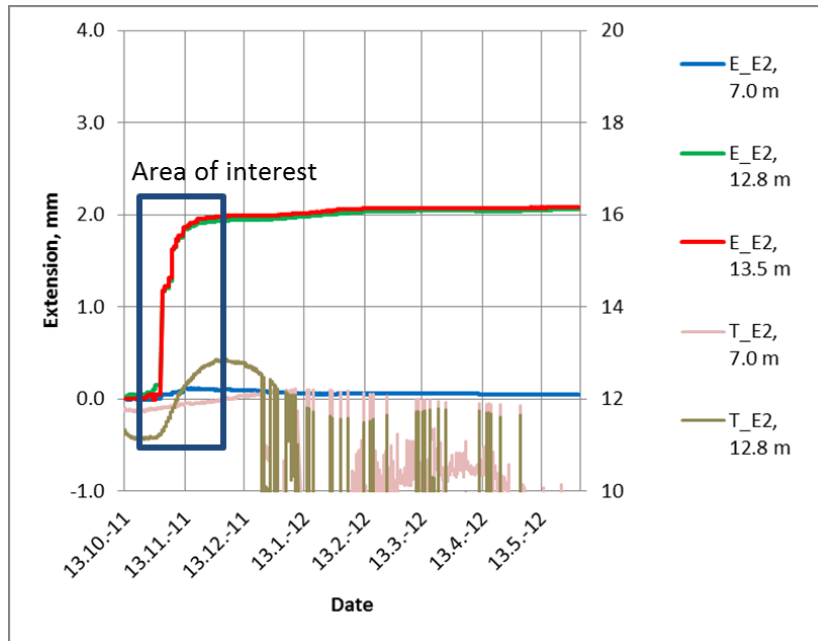


**Figure 30. Time frame of interest of the Posiva measurements. Extensometers marked with E\_EX and temperature measurements as T\_EX. (Siren T. 2013)**

The second task after picking the data was to convert the measured displacements into strains. This was done as previously because the rod extensometers used at the Posiva test site worked similar to previously used Smart MPBXs, only the locations of the anchor heads of the extensometers were at different length.

The measured strains varied from  $10\text{E}-8$  to  $10\text{E}-4$ . The most significant changes occurred at the end of October and in the beginning of November. After the first week of November the change speed of the strains slowed down.

**Table 11. Strains of the chosen measured displacements.**

	<i>EXTP- 1/(7.0m)</i>	<i>EXTP- 1/(12.8m)</i>	<i>EXTP- 1/(13.5m)</i>	<i>EXTP- 2(7.0m)</i>	<i>EXTP- 2(12.8m)</i>	<i>EXTP- 2(13.5m)</i>
13.10.2011 0:27	0.00E+00	0.00E+00	0.00E+00	0.00E+00	0.00E+00	0.00E+00
23.10.2011 5:00	1.18E-06	2.87E-06	8.03E-07	-8.54E-07	3.85E-06	4.98E-07
26.10.2011 23:00	2.19E-07	3.96E-06	1.23E-06	-1.03E-06	5.35E-06	3.10E-06
27.10.2011 23:00	4.16E-06	4.52E-05	4.30E-05	-2.17E-07	7.72E-06	-7.02E-07
28.10.2011 23:00	4.30E-06	5.04E-05	4.89E-05	-2.01E-07	1.17E-05	3.40E-06
31.10.2011 23:00	5.51E-06	5.46E-05	5.27E-05	1.16E-06	1.82E-05	9.49E-06
1.11.2011 23:00	1.14E-05	1.13E-04	1.15E-04	6.27E-06	9.12E-05	8.73E-05
4.11.2011 23:00	1.16E-05	1.24E-04	1.28E-04	6.74E-06	1.00E-04	9.72E-05
6.11.2011 23:00	1.47E-05	1.37E-04	1.41E-04	1.00E-05	1.26E-04	1.21E-04
8.11.2011 23:00	1.46E-05	1.40E-04	1.46E-04	1.03E-05	1.34E-04	1.28E-04
12.11.2011 23:00	1.49E-05	1.52E-04	1.55E-04	1.61E-05	1.44E-04	1.38E-04
16.11.2011 23:00	1.44E-05	1.55E-04	1.58E-04	1.57E-05	1.47E-04	1.42E-04
20.11.2011 23:00	1.39E-05	1.58E-04	1.60E-04	1.55E-05	1.49E-04	1.45E-04
18.12.2011 23:00	1.16E-05	1.60E-04	1.63E-04	1.26E-05	1.52E-04	1.48E-04

The modelling of the Posiva test site was done using two-staged model. The two stages of the modelling are showed in Figure 31. In the first stage the displacements caused by the earlier excavation were modelled. In the second stage the displacements caused by the target excavation were modelled. After this the displacements caused by the earlier activities were deducted from the stage two displacements.

The load cases were formed as for the Kylylahti mine analysis. The parameters used for the modelling are showed in Table 12. The used rock mass modulus ( $E_m$ ) is typical value used at the ONKALO test site when joints are not modelled separately and it has to be noted that it is significantly higher than the  $E_m$  used for the Kylylahti mine analysis.

The modelled strains are shown in Table 13, Table 14 and Table 15. For  $\sigma_1$  the modelled strains were higher than the highest measured displacements which was expected because the load cases were formed using 100 MPa loads. The  $\sigma_2$  load case strains were all negative and in the  $\tau_{xy}$  load case the strains were within same region as the measured strains

**Table 12. Modelling parameters for the Posiva test site. (Hakala. Valli. 2013. p. 7)**

<i>Parameters</i>	<i>Value</i>	<i>Unit</i>
<i>Rock Mass Modulus (<math>E_m</math>)</i>	53	GPa
<i>Poisson Ratio</i>	0.25	

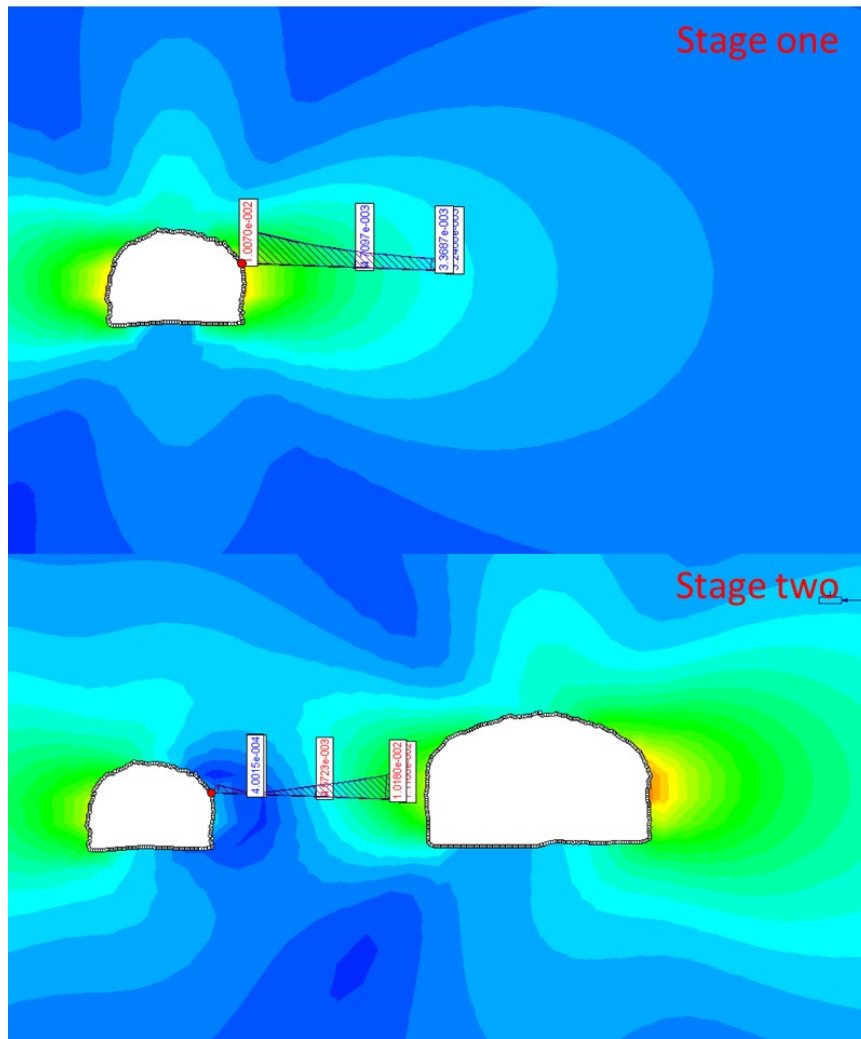


Figure 31. Modelled stages at the Posiva test site.

Table 13: Modelled strains for the Posiva test site.  $\sigma_1$ .

	<i>Ext-L</i>	<i>Ext-I</i>
7 m	0.000284	0.000299
12.8 m	0.000546	0.00056
13.5 m	0.00057	0.000604

Table 14. Modelled strains for the Posiva test site.  $\sigma_3$

	<i>Ext-L</i>	<i>Ext-I</i>
7 m	-0.00014	-0.00015
12.8 m	-0.00016	-0.00017
13.5 m	-0.00011	-0.00015

**Table 15. Modelled strains for the posiva test site. Tau**

	$\tau_{xy}$	
	Ext-L	Ext-I
<i>7 m</i>	0.000148	0.000182
<i>12.8 m</i>	9.29E-05	0.000132
<i>13.5 m</i>	7.85E-05	0.000126

The results from the algorithm are shown in Table 16 and Table 17. The first table shows how the beta factors gained from the multiple linear regression act. The Beta1 factors gains its highest relative change between 31<sup>st</sup> of October and 1<sup>st</sup> of November. The Beta2 and Beta3 both gained their highest relatives changes already between the 26<sup>th</sup> and 27<sup>th</sup> of October.

The results are plotted against time in Figure 32. In this plot it is more clearly presented that the change of  $\sigma_1$  happens in two steps. Figure 33 and Figure 34 show how the fits behave when displacements start occur. As with Kylylahti mine data, when the displacements increase the fits improve.



**Table 16. Beta factors of the multiple linear regression analysis of the Posiva data.**

<i>Results</i>	<i>Beta1</i>	<i>Beta2</i>	<i>Beta3</i>
13.10.2011 0:27	0.00	0.00	0.00
23.10.2011 5:00	-0.75	-8.63	-6.10
26.10.2011 23:00	-0.25	-7.82	-6.40
27.10.2011 23:00	1.37	-41.39	-41.21
28.10.2011 23:00	2.56	-41.94	-43.82
31.10.2011 23:00	3.45	-42.91	-45.17
1.11.2011 23:00	19.88	-39.61	-65.38
4.11.2011 23:00	22.80	-38.46	-69.39
6.11.2011 23:00	26.68	-38.32	-72.71
8.11.2011 23:00	28.50	-34.67	-72.16
12.11.2011 23:00	29.99	-38.39	-75.94
16.11.2011 23:00	30.88	-38.77	-78.02
20.11.2011 23:00	31.59	-38.49	-79.12
18.12.2011 23:00	32.59	-39.00	-82.72

**Table 17. Final results of the Posiva test site near field analysis.**

<i>Results</i>	$\sigma_1$ (MPa)	$\sigma_3$ (MPa)	$\varphi$ (°)
13.10.2011	0.00	0.00	0.00
23.10.2011	2.57	-11.96	61.43
26.10.2011	3.40	-11.47	60.30
27.10.2011	26.42	-66.43	58.71
28.10.2011	29.46	-68.83	58.46
31.10.2011	31.04	-70.50	58.58
1.11.2011	61.97	-81.69	57.23
4.11.2011	68.02	-83.68	56.91
6.11.2011	73.82	-85.46	57.04
8.11.2011	75.68	-81.85	56.82
12.11.2011	79.08	-87.48	57.12
16.11.2011	81.49	-89.39	57.03
20.11.2011	83.08	-89.99	56.94
18.12.2011	86.93	-93.34	56.70

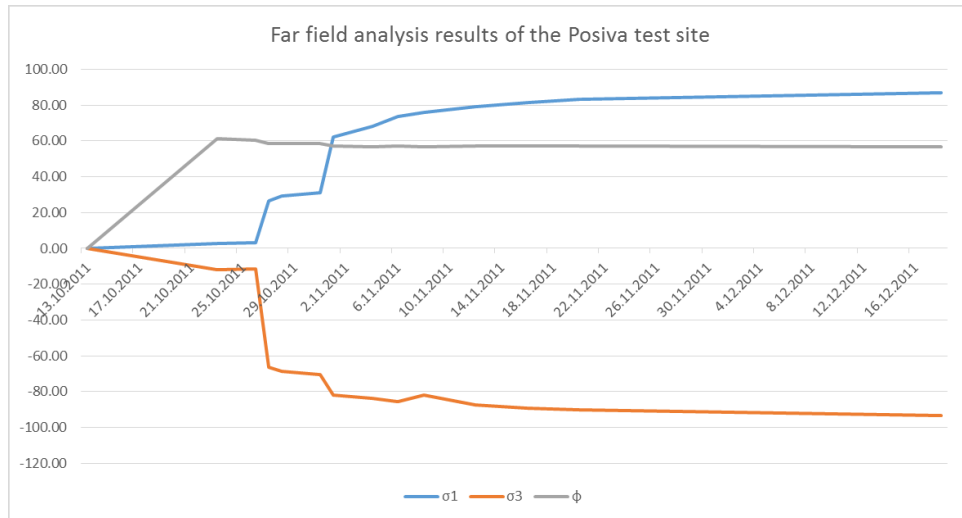


Figure 32. Posiva test site results against time.

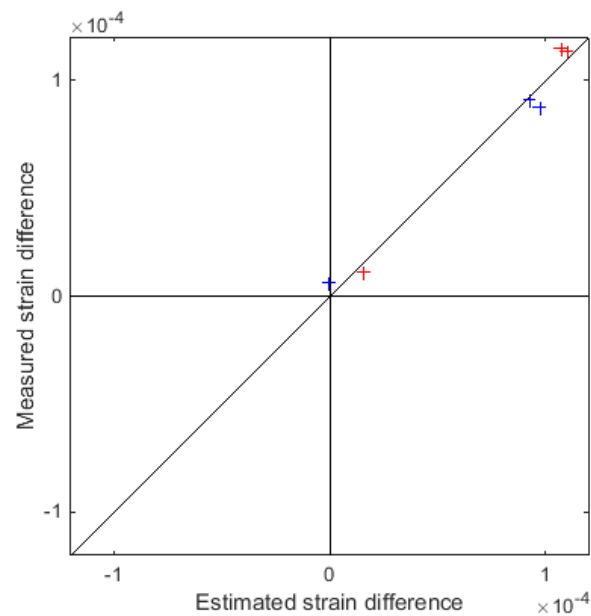
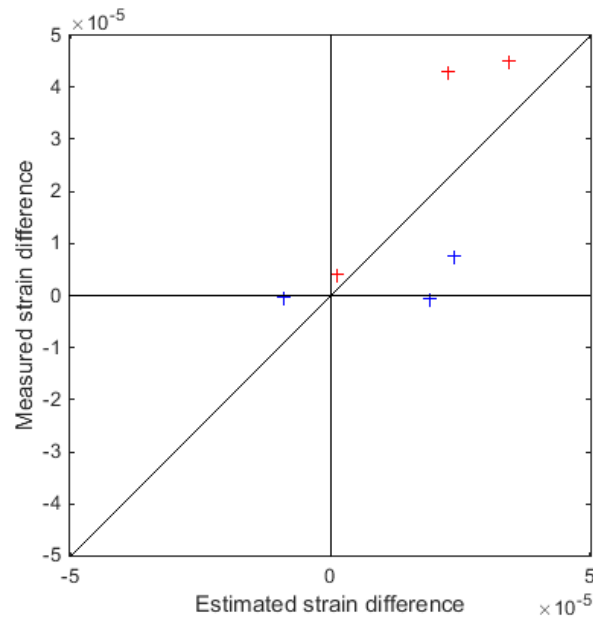


Figure 33. The fit on 1<sup>st</sup> of November 2011 between measured and estimated strains. Extensometers marked with different colors.



**Figure 34. The fit on 27<sup>th</sup> of October 2011 between measured and estimated strains. Extensometers marked with different colors.**

## 6 Discussions

In the discussions main reasons affecting the results gained from algorithm are covered. Also improvements for the future are presented. The main concentration in the discussions is aimed to understand the most problematic areas when using the algorithm presented in this study.

As conclusion it can be said that algorithm gives high values for the stress change. Main target of the conclusions is to walk through reasons which are affecting to the behavior of the results gained from the multiple linear regression analysis.

The main reasons affecting to the results are all covered separately in the conclusions. These reasons are joints crossing the extensometers, affect and accurate determination of the rock mass modulus ( $E_m$ ) and Poisson's ratio, Type of used measurement equipment and different modelling software.

### 6.1 *Joints*

As was already discussed previously in this study, opening or closing joints cause displacement in a manner that harms the results gained from the algorithm. The mechanism is showed in Figure 35. In this case the joint at the beginning of the multipoint borehole extensometer is affecting to all of the separate rods with same displacement. This causes the strains of the first extensometers to grow higher than what the models indicate thus giving bad fits and results from the algorithm.

This problem could be overcome with more detailed modelling and instrumentation process. The displacement of the first extensometer could be deducted from the other extensometers enabling reliable and useful readings to be used from them. In this case the first part of the MPBX would have to be discarded. This proposed method also re-

quires that location of possible joints are investigated from the boreholes prior to installation. This solution would not require modelling of the joints but would require more extensive instrumentation.

Other possibility to overcome this problem is to model the impact of the joints. In this case precise location, dip, direction and the needed joint parameters would have to be known and investigated. This kind of data is not usually gathered from mine sites thus the solution is impractical. For the purpose of the algorithm both solutions are usable but for quicker analysis eliminating the joint would be more beneficial.

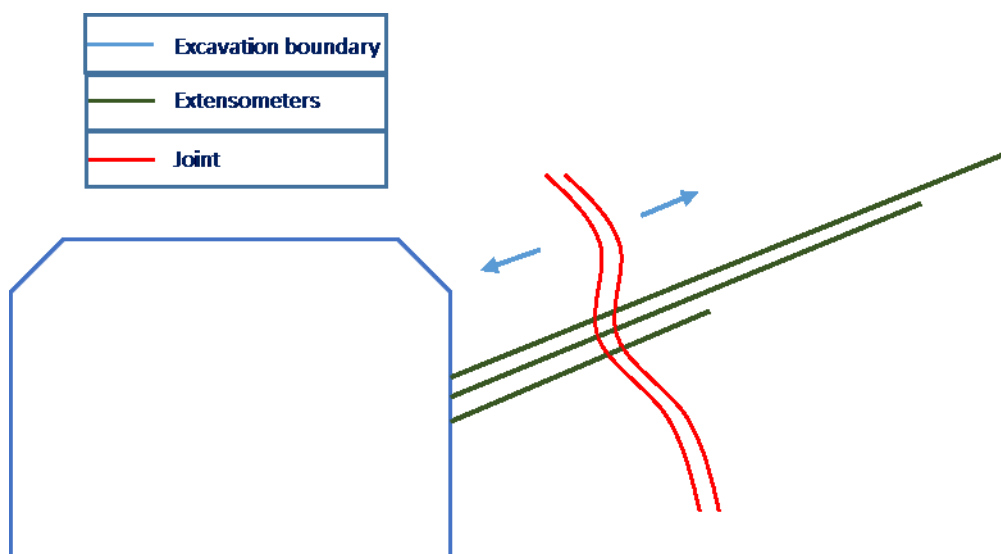


**Figure 35. Impact of joint to multipoint borehole extensometer.**

It would have greatly contributed to this study if the boreholes would have been documented more precisely in Kylylahti. The borehole data was also missing from ON-KALO. This documentation should have included mapping of geological structures within the borehole with any current technique. This would have helped to recognize error sources in the measurements.

The joints affecting the measurement can be spotted from the data if they are located as presented in Figure 35. The strains received from the measurements are most affected in short distances from tunnel. This causes the results of the algorithm to fit into curve instead of a line (See Figure 36).

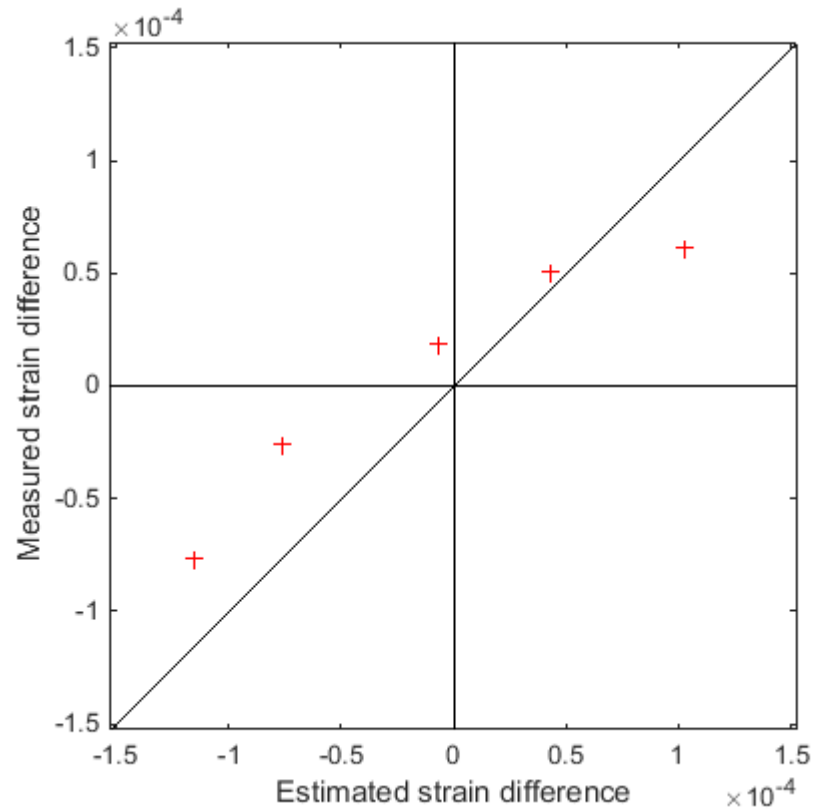


**Figure 36. Joint example. Joint causing the curvature due to the fact that most of the displacements are in on place.**

If the rock mass is already disturbed and especially if there has been stopes mined near the measurement area, there might be joints which have already opened. This increases the necessity of monitoring the measurement boreholes with care. The opened joints might close down during mining the target stope of the study and thus impact to the results of the measurement. Closing joints might also harm the instruments. This is discussed more detail in chapter 6.3.

The effect of a joint is presented in Figure 37 as spring system. In reality the spring system has two spring coefficients, one from the joint and one from the rock mass itself. This only applies to compression since the joint is thought not to have tensile strength. As can be seen from formula 5 the two coefficients can be combined. In this case if one of the coefficients is much higher than the other, the lower one is mainly affecting to the system. The usual case is that the joint coefficient is much lower than the coefficient from the rock mass, thus the joint is mainly affecting to the system.

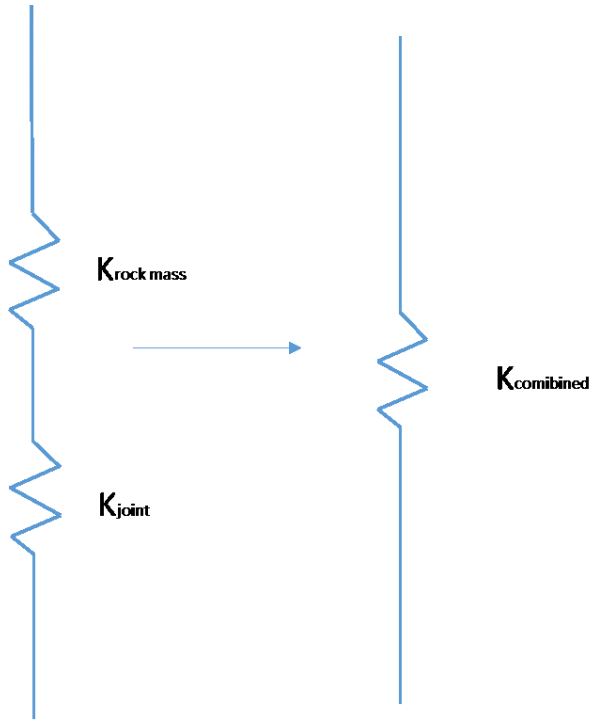


Figure 37. Effect of joint in rock mass presented as one-dimensional spring.

$$k_{combined} = \frac{1}{\frac{1}{k_{rm}} + \frac{1}{k_j}} \quad (5)$$

## 6.2 Rock mass modulus and Poisson ratio

Precise determination of rock mass modulus ( $E_m$ ) and Poisson's ratio ( $\nu$ ) is vital for the study. Both of the parameters influence the results of the algorithm linearly and are connected to each other. The relationship between  $E_m$  or Young's modulus and strain and stress is showed in Equation  $\varepsilon = \frac{\Delta\sigma}{E_m}$  where,  $\varepsilon$  is the strain caused by the change of the stress state,  $\Delta\sigma$  is change of the stress state and  $E_m$  is Young's modulus or rock mass modulus. Rock mass modulus has been used in this study.

The equation to calculate the rock mass modulus used in this study is shown in the next sentence. The equation is presented in article from Hoek and Brown (1997) as following  $E_m (MPa) = E_i(0.02 + \frac{1 - \frac{D}{2}}{60 + 15D - GSI})$  where  $E_m$  is rock mass modulus,  $E_i$  is intact modulus of elasticity,  $D$  is disturbance factor and  $GSI$  is geological strength index. For

both sites examined in this study these factors were previously determined by consultant companies or by the company itself.

As said, the accurate determination of the rock mass modulus is vital to gain accurate results from the algorithm. When the GSI is determined it should be determined from the boreholes used for the measurement devices. This way it can be ensured that the GSI represents the area in the interest of the measurements. Also drill cores can be used to determine the GSI if the holes are made with core drill.

The algorithm could be also used to determine rock mass modulus if it is combined with stress measurements. This way the stress change is known in the algorithm but the rock mass modulus is set to be the unknown parameter.

Some of the problems related to determining the rock mass modulus could possibly be solved by using more sophisticated modelling software. This is discussed in more detail in chapter 6.4.



### 6.3 *Used measurement equipment*

The used measurement equipment worked well under harsh conditions. The dataloggers and the extensometers were placed near the excavation, especially at the test site number two.

In total it can be said that the measurement equipment are accurate enough to provide reliable data for the algorithm. Exception was the manual readout unit used in the Kylahti mine. The manual readout had resolution which impacted to the results gained from the algorithm.

Special care for choosing, placing and installing the measurement units has to be taken. This study relayed to one measurement equipment type and that can be seen as mistake as MPBX extensometers are not able to measure compression unlike conventional extensometers. Use of traditional extensometers would probably have increased the reliability of the results, especially at the 3D test site where also compression driven displacements occurred.

The installation pattern, especially at the test site two was not optimal. The installation would probably have been easier if the extensometers could be installed into downholes instead of upholes. This was considered already during the planning of the installations but there was no possibility to use downholes. With downholes the pumping of the cement is more reliable and can be done with lower hose pressure.

If the directions and magnitude of displacement is known prior to installation the measurement equipment used in this study are sufficient. The magnitude of the displacement is important to know to ensure that the extensometers are equipped with proper strokes. The direction has to be known to ensure that the equipment can be placed so that they are placed into area where tension driven displacements occur.

To gain full confidence to the measurements it is suggested by the experience gained in this study to combine several measurement equipment types to solve problematic re-

sults. One of the main reasons to abandon further investigations of the Kylylahti measurement site two data was that data included compression driven displacements. The used equipment cannot accurately measure these displacements.

Possibility to overcome this problems is to include conventional extensometer capable of measuring also compression into the instrumentation.

To gain more confidence to the results gained from the extensometer measurements comparison to CSIRO HI (Hollow Inclusion) cell or similar strain cell measurements would have been sensible. If the algorithm is tested in the future, the measurements used in this study should be combined with strain cell measurements. In this study combining extensometers with CSIRO HI cells was thought but the idea was abandoned due to budget restrictions. Retrospectively this was not a good decision.

#### 6.4 ***Modelling and software used for the modelling***

In this study main modelling software used was Examine2D. Examine 2D is modelling software acting plainly under elastic medium restrictions. Other possibilities were considered in earlier stage of the Dynamine project but Examine was seen as a good solution for early stage testing of the method.

Restrictions of the Examine are discussed previously in this study. The main consideration of this chapter is to consider possibilities of more sophisticated modelling methods.

The main pros using Examine were fast calculation of the model, usability and that it had been used in the previous part of the Dynamine project. Examine also provides chance for quick alternations of the model because it only uses the excavation boundaries

The main interest for the study is to model the rock mass as accurately as possible. In Examine2D and with boundary element method in general the rock mass is described with only two parameters, Poisson's ratio and rock mass modulus. This does not provide chances to model the rock mass accurately, especially because the joints were not modelled separately but were included into the rock mass modulus.

Finite element method (FEM) programs such as Rocsciences RS<sup>2</sup> and RS<sup>3</sup> would have given a possibility to use several rock mass domains. This would have increased the accuracy of the modelling but would have required more precise determination of location of different rock units. Using FEM programs would have also increased calculation time of the load cases but this can't be seen having great impact for the study.

Lately new methods to model rock mass have been developed. Modelling approaches such as presented in article by Ivars et. al. (2011) would suit the algorithm well. Especially at the 3D test site at the Kylylahti mine this kind of modelling approach would have been needed due the disturbed rock mass.

The synthetic rock mass approach presented in the article is designed for scales from 10 m to 100 m. This suits well for the purposes of this type of study. The synthetic rock mass combines discrete fracture network (DFN) with intact rocks bonded particle model. The cons of this type of modelling would be increased time to create the model and the increased calculation time of the model. The model would also require more input data of the fracture network and joints included into modelled area.

## **6.5 *Improvements for installation procedure***

To improve the measurement method in the future studies some improvements are proposed. The drillholes should be monitored prior to installation. The best solution for the monitoring of the drillholes would be to measure the deviation using electromagnetic surveying (EMS) and to do optical borehole imaging (OBI) inside the borehole to reveal rock mechanical structures affecting the study. Both measurements were considered to be too expensive for the project.

For the analysis both measurements would have given valuable information. EMS would have enabled more accurate modelling input for the placement of the extensometer. The OBI would have given information of the homogeneity of the rock mass within the extensometers region and also information of potential error source such as joints.

Also, there had been no extensometer installations before at the Kylylahti mine and some improvement suggestions for future installations were presented:

1. Using a concrete truck instead of Robolt would decrease the installation time when installing multiple extensometers.
2. Thickness and durability of the grouting hose should be sufficient for installation to avoid unnecessary break-downs of equipment. The grouting hose should be kept in warm warehouse because the temperature changes can cause wearing of the material
3. Downhole installations should be done whenever possible to ease up the installation. Upholes require more pressure from the grouting pump and thus take more time. In this case downholes were not possible due to blockages at upper level.

## 7 Conclusions

In this chapter conclusions based on this study are presented. The main considerations are in the suitability of the method to mining environment and in problems which occurred during the study. Also proposals for future studies are presented.

The algorithm works well with synthetic data. In this study testing of the algorithm with synthetic data analysis was not excessive. It was done to verify that the work done previously was suitable for test in real mining environment and to ensure that the previously done synthetic analysis were accurate. The error in the synthetic analysis varied from less than one percentage to over three percentage. This was thought to be accuracy level which was acceptable to move on to the real data analysis and it proved that in theory the method works for elastic rock mass. It has to be noted that CHILE rock conditions were assumed for the synthetic data analysis.

The method of forming the different load cases ( $\sigma_{xx}$ ,  $\sigma_{yy}$  and  $\tau_{xy}$ ) was also concluded to be suitable for the study. The used method was chosen because it was fast to execute using Examine2D modelling program and proved to provide reliable results from the synthetic data analysis.

The results gained from the Kylylahti measurements were not satisfactory. The magnitude of the results is too high to be reliable especially at the end of the measurement period. The near field analysis gave the best results and the near field analysis can be interpreted to be fairly reliable until to the last measurement.

The two different modelling methods, near and near field modelling, also differ from each other considerably. The far field analysis gave higher results than the near field analysis. This was thought to originate from the fact that the stope mined next to the measurement area was within near field radius of the model. The distance from the measurement area to the stope was approximately three times the radius of the tunnel but the closest measurement points were only 10 meters from the stope.

The data gained from Posiva was more consistent and included more data points than the data received from Kylylahti mine measurements. The direction of the displacement was constant and was according to the models done prior to the installations.

The negative part of the measurements was that it only included six measurement points and the two extensometers were installed to the same direction so that the displacements occurring perpendicular to the extensometers were not spotted. More extensometers with more representative installation pattern would have increased the reliability of the results.

Both of the near field analysis, for the ONKALO and Kylylahti test sites, provided similar results. These results were too high to be reliable. On the other hand the algorithm was able to spot when the stress state changes occurred.

It can also be concluded that using far field analysis in this kind of test setting provides more unsatisfactory results than using the near field analysis. The results gained from the far field analysis were even in the higher magnitude than the results gained from near field analysis.

At the current development stage the algorithm is not usable in mining environment. The most important factors impacting to the usability of the algorithm are:

- Displacements or strains caused by plastic deformation
- Earlier activities at the level in Kylylahti mine which caused the rock mass to be disturbed in the beginning
- Over estimated modelling parameters such as Rock Mass Modulus and Poisson's ratio.
- Using of linearly elastic model
- Measurement inaccuracies.
- Readout inaccuracies

For further studies these factors have to be considered. The next step for this study would be to replicate the 2D test site with improvements. These improvements would be documentation of the boreholes, using a model capable of dealing with plasticity, more precisely investigated rock mass at the area, increasing the amount and variety of instruments and comparison study using CSIRO hollow inclusion cell.

## References

- Bawden W.F. & Tod J.D. 2002. Validation of Cable Bolt Support Design in Weak Rock Using SMART Instruments and Phase2. <http://www.roscience.com/library/roc-news/june2002/Validation.pdf>.
- Bergström P., Sahala K., Hakala M. 2014. From High stressed to de-stressed – mining in changing conditions. Deep Mining 2014. ISBN 978-0-9870937-9-0
- Dulmage A. 1.9.2014-31.5.2015. Personal communication.
- Hakala M., Valli J. 2013. ONKALO POSE experiment – Phase 3: 3DEC prediction. [http://www.posiva.fi/files/3160/WR\\_2012-58.pdf](http://www.posiva.fi/files/3160/WR_2012-58.pdf)
- Hoek E., Brown E.T. 1997. Practical estimates of rock mass strength. International Journal of Rock Mechanics and Mining Sciences. Vol. 34, Issue 8. Pp. 1165-1186.
- Hoek E., Kaiser P.K., Bawden W.F. 2000. Support of underground excavations in hard rock. CRC Press. 215p. ISBN: 978-9054101871.
- Inverse Problem Research. 2015. Finnish Center of Excellence in Inverse Problem Research. <http://wiki.helsinki.fi/display/inverse/Home>.
- Ivars, D., et al. 2011. "The synthetic rock mass approach for jointed rock mass modelling. International Journal of Rock Mechanics and Mining Sciences 48.2 : pp. 219-244.
- Jing, L., Hudson, J. A. Numerical methods in rock mechanics. 2002. International Journal of Rock Mechanics and Mining Sciences, v. 39, n. 4, p. 409-427, 6// 2002. ISSN 1365-1609.
- Kaiser P.K., Yazici S., Maloney S. 2001. Mining-induced stress change and consequences of stress path on excavation stability - a case study. International Journal of Rock Mechanics & Mining Sciences 38. Pp.167–180.

Kodeda S. 2015. Master's thesis: Stress state change estimation using back calculation of strain sensor data. Unpublished.

Kodeda S., Ritala F., Siren T., Uotinen L. 2015. Real time stress change estimation using strain measurements. EUROCK 2015 & 64th Geomechanics Colloquium. Schubert (ed.).

Rocscience. 2015. Examine 2D product description. <https://www.rocsience.com/products/11>

Shen B., King A., Guo H. 2008. Displacement, stress and seismicity in roadway roofs during mining-induced failure. International Journal of Rock Mechanics & Mining Sciences 45. Pp. 672- 688.

Siren T. 2012. Results of Monitoring at Olkiluoto in 2012. Working Report 2012-47. Posiva Oy, Olkiluoto.

Siren T. 2013. Results of Monitoring at Olkiluoto in 2013. Working Report 2013-47. Posiva Oy, Olkiluoto.

Tod J. & Lausch P. 2002. Interpreting and Troubleshooting SMART Instrumentation. Mine Design Technologies Inc.



## Appendices

### Appendix 1: Total displacements and the comparison displacements

<i>Angle of the query (Deg.)</i>	<i>Total Displacement (mm)</i>	<i>Comparison displacement (mm)</i>
0	3.4	2.1
5	3.1	2
10	2.3	1.9
15	2.7	2.1
20	1.9	1.8
25	1.5	1.5
30	1.1	1.3
35	0.3	0.8
40	0.7	1
45	-0.1	0.4
50	0	0.6
55	-0.7	-0.1
60	-1.2	-0.4
65	-1	-0.3
70	-1.4	-0.6
75	-1.6	-0.7
80	-1.6	-0.8
85	1.8	2.7
90	-1.9	-1

### Appendix 2: Measured strains from Kylylahti mine

	<i>0 to 3.33</i>	<i>0 to 6.66</i>	<i>0 to 10</i>	<i>0 to 13.33</i>	<i>0 to 16.67</i>	<i>0 to 20</i>
27.12.2014	0.00E+00	0.00E+00	0.00E+00	0.00E+00	0.00E+00	0.00E+00
31.12.2014	-7.62E-05	-3.81E-05	-2.54E-05	-1.91E-05	-1.52E-05	-1.27E-05
1.1.2015	-7.62E-05	-3.81E-05	-2.54E-05	-1.91E-05	-1.52E-05	-1.27E-05
5.1.2015	-7.62E-05	-3.81E-05	-2.54E-05	-1.91E-05	-1.52E-05	-1.27E-05

12.1.2015	0.00E+00	0.00E+00	0.00E+00	-1.91E-05	0.00E+00	0.00E+00
22.1.2015	0.00E+00	0.00E+00	2.54E-05	0.00E+00	0.00E+00	0.00E+00
9.3.2015	3.05E-04	1.52E-04	2.54E-05	-1.91E-05	-3.05E-05	-3.81E-05

### Appendix 3: Measured displacements from ONKALO

	EXTP- 1/(7.0m)	EXTP- 1/(12.8m)	EXTP- 1/(13.5m)	EXTP- 2(7.0m)	EXTP- 2(12.8m)	EXTP- 2(13.5m)
13.10.201 1 0:27	0.000	0.000	0.000	0.000	0.000	0.000
23.10.201 1 5:00	0.008	0.037	0.011	-0.006	0.049	0.007
26.10.201 1 23:00	0.002	0.051	0.017	-0.007	0.068	0.042
27.10.201 1 23:00	0.029	0.578	0.580	-0.002	0.099	-0.009
28.10.201 1 23:00	0.030	0.645	0.660	-0.001	0.149	0.046
31.10.201 1 23:00	0.039	0.699	0.711	0.008	0.233	0.128
1.11.2011 23:00	0.080	1.452	1.553	0.044	1.168	1.179
4.11.2011 23:00	0.081	1.591	1.727	0.047	1.280	1.312
6.11.2011 23:00	0.103	1.755	1.905	0.070	1.615	1.628
8.11.2011 23:00	0.102	1.792	1.965	0.072	1.717	1.733
12.11.201 1 23:00	0.105	1.944	2.089	0.113	1.841	1.861
16.11.201 1 23:00	0.101	1.990	2.132	0.110	1.879	1.915
20.11.201 1 23:00	0.097	2.019	2.163	0.108	1.911	1.953
18.12.201 1 23:00	0.081	2.050	2.198	0.088	1.947	1.993

### Appendix 4: Used algorithm

```
f=fullfile('2d_mpbx_versio2.xlsx'); %% Inserting the file with meas-
ured strains
```

```
xlstrange='c11:h11'; %%Taking the strains of the first extensometer
xl1=xlsread(f,'Sheet1',xlstrange);
strain_1=rot90(xl1);
strain_1=xl1';
```

```
xlstrange='C21:h21'; %%Taking the strains of the second extensometer
xl2=xlsread(f,'sheet1',xlstrange);
strain_2=rot90(xl2);
```

```

strain_2=x12';

Y(1:6,1)=zeros; %% Forming of matrix from the measured strains
Y(1:6,1)=strain_1
Y(7:12,1)=strain_2

file=fullfile('near_field_case_versio2.xlsx'); %% Inserting the file
with modelled strains. After this the load cases for both of the ex-
tensometers are fetched

xlsrange='b5:b10';
MalliSig1a=xlsread(file,'sheet1',xlsrange);
xlsrange='C5:C10';
MalliSig1b=xlsread(file,'sheet1',xlsrange);
xlsrange='e5:e10';
MalliSig2a=xlsread(file,'sheet1',xlsrange);
xlsrange='f5:f10';
MalliSig2b=xlsread(file,'sheet1',xlsrange);
xlsrange='H5:H10';
MalliTaula=xlsread(file,'sheet1',xlsrange);
xlsrange='i5:i10';
MalliTau2b=xlsread(file,'sheet1',xlsrange);

scale = 100;

X(1:12,2)=zeros; %% Forming the matrix from the load case displace-
ments
X(1:6,1)=MalliSig1a/scale;
X(7:12,1)=MalliSig1b/scale;
X(1:6,2)=MalliSig2a/scale;
X(7:12,2)=MalliSig2b/scale;
X(1:6,3)=MalliTaula/scale;
X(7:12,3)=MalliTau2b/scale;

beta=(X'*X)^(-1)*(X'*Y) %% Calculating the beta factors with ordinary
least square method

estimate=X*beta %%variable used to comapre measured and modelled
strains

figure %% Forming of the comparison figure
plot(estimate(1:6),Y(1:6),'r+',estimate(7:12),Y(7:12),'b+')
axis square
axis_max = max([abs(max(max([estimate Y]))+ 0.00005) min(min([estimate
Y])-0.00005)]);
axis([-axis_max axis_max -axis_max axis_max])
line([-axis_max axis_max], [-axis_max axis_max], 'Color', 'k');
line([0 0], [-axis_max axis_max], 'Color', 'k');
line([-axis_max axis_max], [0 0], 'Color', 'k');
xlabel('Estimated strain difference')
ylabel('Measured strain difference')

```

```
dev=((beta(1)-beta(2))/2); %% After this the results are transformed
using the cauchy equations
angle=(atan(beta(3)/dev))/2/pi*180;

if (angle < 0)
    angle = angle + 90;
end

coef=power(power(dev,2)+power(beta(3),2),0.5);

avr=((beta(1)+beta(2))/2);

sig_1=avr+coef;
sig_3=avr-coef;

result(:,1)=[sig_1,sig_3,angle]
```